Sl. No.	IIT Ropar List of Recent Publications with Abstract Coverage: December, 2023
1.	2310P oxygen nano-bubbles attenuate hypoxia-induced tumour malignancy in tumour xenograft models K Bhavya…**Y Singh, NN Nirmalkar, D Pal** - Annals of Oncology, 2023 **Abstract:** Background: The rapid proliferation of cancer cells leads to abnormal vascularization, creating a hypoxic tumor core in most advanced solid tumors. Recent studies have shown that hypoxia is associated with poor prognosis in cancer patients. Tumor aggressiveness is driven by hypoxia, which confers resistance to many conventional cancer therapies. In the present study, we propose that oxygen nanobubbles can reduce the hypoxic effect on the epithelial-to-mesenchymal transition (EMT) and prevent migration and invasion in non-small cell lung cancer (NSCLC) and triplenegative breast cancer (TNBC). Methods: Using the sonic cavitation method, we have developed a method to generate bulk oxygen nanobubbles (ONBs) with dipalmitoyl phosphatidylcholine (DPPC) lipid and quantitate mean diameter and number density through nanoparticle tracking analysis and insight. We have treated A549 lung adenocarcinoma and MDAMB-231 triple-negative breast cancer cell lines with 1% oxygen and ONB. We have also checked its preventive role in the zebrafish tumor xenograft model. We have measured HIF-1a and EMT expression markers by immunoblot and qPCR analysis. Moreover, we have used the 4T1 BALB/c mice tumor xenograft model for further confirmation. Results: ONB promotes HIF-1a hydroxylation and its proteasomal degradation in hypoxic cancer cells. ONBs treated A549 and MDA-MB-231 cancer cells and an adult zebrafish A549 tumor xenografts showed the downregulation of TGF-b and VEGFA expression at the transcriptional and translational levels, which also led to upregulation of epithelial genes like E-cadherin with down-regulation of mesenchymal genes like N cadherin, Vimentin, Fibronectin. ONB treatment significantly affects cancer cell migration. Also, liposomal ONB administrated 4T1 BALB/c breast tumor xenograft model showed similar results. Conclusions: ONBs reduce HIF-1 mediated epithelial to mesenchymal transition (EMT) controlled by TGF-b and VEGFA and prevent cellular migration and invasion in solid tumors, particularly NSCLC and TNBC. In conclusion, targeted administration of ONB could be a better therapeutic approach to inhibit the hypoxic detrimental effect, which helps to increase the efficacy of anticancer treatments.
2.	A compact stacked multisector near-isotropic coverage rectenna array system for iot applications **S Kumar, M Kumar, A Sharma** - IEEE Microwave and Wireless Technology Letters, 2023 **Abstract:** A low-profile, fully integrated, eight-sector rectenna array is proposed to achieve near-isotropic coverage for an angular misalignment-tolerant wireless power transfer (WPT) system. The proposed design incorporates a new Schottky diode connection strategy to simplify the integration of the rectenna elements (ReEs). The system utilizes a hybrid combining topology and conjugate impedance matching of ReEs with Schottky diode impedance. This reduces circuit losses and enhances system power conversion efficiency (PCE). Additionally, the hybrid combining scheme improves the output dc voltage and the optimal load. Moreover, the sustainable battery-less operation of a wireless sensor node is realized by employing a power management unit (PMU) with the proposed system.
3.	A detailed investigation and catalytic application of gold nanoparticles towards synthesis of N & O-heterocycles S Chakroborty, J Malviya…**NP Mishra**… - Topics in Catalysis, 2023

	Abstract: Nanotechnology advancements, notably in catalysis, have found several uses in the fabrication of heterocyclic molecules. An abundance nanoparticle (NPs) has been successfully used in a variety of organic transformations, which prompted us to undertake concentrated efforts to cover all instances in which gold nanoparticles (Au NPs) have been used in organic transformations. The catalytic application of gold nanoparticles in organic transformation has gained considerable interest researchers owing to its physical and chemical properties. Gold nanoparticles as catalysts in organic reactions deliver robust, green, and cost-effective alternatives for the synthetic transformations of heterocyclic scaffolds. Nitrogen- and oxygen-containing heterocyclic atoms are the essential prime units existing in diverse carbon-based vibrant lives and are substantial for industrial, pharmaceutical, and agrochemicals. Our focus will be on Au NP-catalyzed reactions in synthetic transformations for the production of heterocyclic scaffolds containing nitrogen and oxygen heteroatoms documented from 2011 to 2022. From a synthetic standpoint, this review will offer the reader an intrinsic framework for selecting the optimal Au NP catalytic system of importance for the synthesis of the preferred heterocyclic scaffold. 
4.	A novel technique for estimating the location of defect or inception of water treeing in the semiconducting screen of a cable **A Das, CC Reddy** - IEEE Transactions on Industrial Electronics, 2023 **Abstract:** In this article, a novel method to estimate the location of a defect in the semiconducting layer either for insulation or the conductor screen of a cable is proposed using broadband impedance spectroscopy through sweep frequency response analysis. A relationship between the sum of frequencies of zeroes and the electrical parameters of the cable is established, perhaps for the first time in the case of a cable. Transmission line theory and state-space model are used to establish the relationship of zeroes with the propagation constant and electrical parameters of the cable, respectively. Furthermore, an analytical formula is proposed for the estimation of the location of defects of various sizes in the semiconducting layer using the frequency location of zeros and their cumulative sum and product. Both, finite element method (FEM)-based simulations, as well as experiments on a test cable, were performed to validate the proposed formulae.
5.	Advances and challenges in nanomaterial-based electrochemical immunosensors for small cell lung cancer biomarker neuron-specific enolase **D Mehta, D Gupta, A Kafle, S Kaur, TC Nagaiah** - ACS Omega, 2023 **Abstract:** Early and rapid detection of neuron-specific enolase (NSE) is highly significant, as it is putative biomarker for small-cell lung cancer as well as COVID-19. Electrochemical techniques have attracted substantial attention for the early detection of cancer biomarkers due to the important properties of simplicity, high sensitivity, specificity, low cost, and point-of-care detection. This work reviews the clinically relevant labeled and label-free electrochemical immunosensors developed so far for the analysis of NSE. The prevailing role of nanostructured materials as electrode matrices is thoroughly discussed. Subsequently, the key performances of various immunoassays are critically evaluated in terms of limit of detection, linear ranges, and incubation time for clinical translation. Electrochemical techniques coupled with screen-printed

	electrodes developing market level commercialization of NSE sensors is also discussed. Finally, the review concludes with the current challenges associated with available methods and provides a future outlook toward commercialization opportunities for easy detection of NSE. 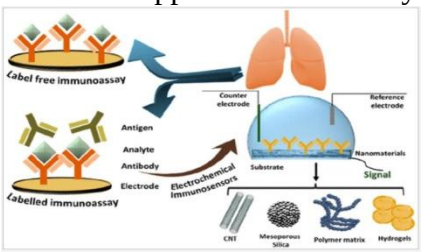
6.	Advancing photovoltaics and optoelectronics: Exploring the superior performance of lead-free halide perovskites M Kibbou, Z Haman…**R Ahuja** ... - Optical Materials, 2024 **Abstract:** One of the emerging directions that has greatly advanced the fields of photovoltaics and optoelectronics is the development of lead-free inorganic halide perovskites. In this study, ab-initio methods were employed to forecast the structural, electronic, and optical behavior of the perovskite materials Cs2Cu+Al3+X6 (where X represents Cl or Br). The analyses conducted have revealed the exceptional structural characteristics of these compounds. The electronic band structure and density of states were computed using the PBE method with the mBJ potential. The direct bandgaps of Cs2CuAlCl6 and Cs2CuAlBr6 were determined to be 1.35 eV and 0.93 eV, respectively. This suitable electrical bandgap results in high visible-light absorption. As a result, the optical characteristics exhibit a significant absorption coefficient (α(ω) ≈1.1×105 cm−1 for Cs2CuAlBr6 and 0.77 ×105 cm−1 for Cs2CuAlCl6), substantial conductivity, and negligible reflectivity (R(ω) < 10%). These attributes render Cs2CuAlCl6 and Cs2CuAlBr6 semiconductors highly appealing for optoelectronic applications. The maximum spectral light conversion efficiency under AM1.5G solar irradiation was assessed by altering the thickness of the structures. The results reveal that the chlorinated perovskite achieves a slightly higher efficiency of 32.72%, whereas the brominated perovskite reaches an efficiency of 29.31%. Despite their remarkably advantageous bandgaps, limited reflectivity, and impressive efficiency, environmentally friendly halide perovskite compounds hold promise as renewable energy conversion materials. This suggests the potential for substantial enhancements in solar cell performance. Furthermore, employing the finite element (FE) method, we performed calculations to assess carrier generation within a specially engineered solar cell structure comprising an environmentally friendly multilayer (CH3NH3SnI3 and Cs2CuAlX6). Our discoveries unveiled an exceptionally elevated total generation rate at the interfaces between CH3NH3SnI3 and Cs2CuAlX6, reaching approximately 2.5 × 1029 m−3/s. These findings offer novel perspectives that contribute to the research community and hold the potential to advance future solar cell systems. © 2023 Elsevier B.V.
7.	Amlex - a smart patient driven oxygen rationing device **A Chander, M Kumar, R Kumar**… **AK Sahani**… - IETE Journal of Research1, 2023 **Abstract:** The COVID-19 virus has severely affected the world in many ways. Especially for poor and developing countries where medical research, technology development, and facilities are at an infant stage. This pandemic had a profound impact on people living in those countries. COVID-19 is a respiratory disease that affects an individual's lungs, leading to suffocation or oxygen deprivation. In conventional systems, a constant flow of oxygen is maintained during both the inhalation and exhalation phases of the patient, which leads to the wastage of oxygen supplied during the exhalation phase. Many studies have shown the reliability and accuracy of the humidity-based detection systems. In the present study, a novel device has been developed to tackle this problem that halts the flow of oxygen from the reservoir when the patient exhales. This is detected by a humidity sensor installed in the mask worn by the patient. An adaptive

	algorithm allows the system to adapt to the different patients and environmental conditions. The prototype has been tested in the lab on multiple individuals, and the system showed satisfactory results by an average saving of 26% of oxygen for all flow rates. This device is very helpful in conserving or optimizing oxygen use.
8.	An edge-cloud infrastructure for weed detection in precision agriculture **A Kaushal**, O Almurshed, A Alabbas, **N Auluck**, O Rana - IEEE International Conference on Dependable, Autonomic and Secure Computing …, 2023 **Abstract:** Accurate identification of weeds plays a crucial role in helping farmers achieve efficient agricultural practices. An edge-cloud infrastructure can provide efficient resources for weed detection in resource-constrained rural areas. However, deployed applications in these areas often face challenges such as connectivity failures and network issues that affect their quality of service (QoS). We introduce a signal quality-aware framework for precision agriculture that allocates weed inference tasks to resource nodes based on the current network connectivity and quality. Two Machine Learning (ML) models based on ResNet-50 and MobileNetV2 are trained using the publicly available DeepWeeds image classification dataset. A rule-based approximation algorithm is formulated to execute tasks on resource-constrained computational nodes. We also designed a testbed setup consisting of Raspberry Pi (RPi), personal laptop, cloud server and Parsl environment for evaluating the framework. Reliability of the framework is tested in a controlled setting, under various dynamically injected faults. Experimental results demonstrate that the proposed setup can accurately identify weeds while ensuring high fault tolerance and low completion time, making it a promising solution for weed management in rural agriculture.
9.	An effective CNN-based method for camera model identification in privacy preserving settings **K Rana, V Rathi, P Goyal** - IEEE International Conference on Image Processing Challenges and Workshops (ICIPCW), 2023 **Abstract:** Recognizing information about the camera model of digital images has been identified as a crucial task in the field of image forensics. Numerous methods have been proposed for camera model identification (CMI), with recent emphasis on convolutional neural networks (CNNs) based methods for their better efficacy. However, current approaches generally consider original images without consideration to privacy preserving aspects. This paper introduces a novel CNN-based approach for CMI even in privacy preserving settings, where unlike conventional approaches, the training and evaluation is performed on encrypted images. For encryption, we consider position scrambling at pixel-level and we also present block-level position scrambling for better efficacy. Experimental results demonstrate the feasibility of our approach in terms of accuracy and privacy preservation. Furthermore, the experiments highlight the effectiveness of our CNN-based approach, having around 10% better accuracy in comparison to traditional statistical models for CMI of encrypted images.
10.	An in situ proton filter covalent organic framework catalyst for highly efficient aqueous electrochemical ammonia production KC Ranjeesh, **S Kaur, D Gupta**…**TC Nagaiah** - Advanced Energy Materials, 2023 **Abstract:** The electrocatalytic nitrogen reduction reaction (NRR) driven by renewable electricity provides a green synthesis route for ammonia (NH_3) production under ambient conditions but suffers from a low conversion yield and poor Faradaic efficiency (F.E.) because of strong competition from hydrogen evolution reaction (HER) and the poor solubility of N_2 in aqueous systems. Herein, an in situ proton filter covalent organic framework catalyst (Ru-Tta-Dfp) is reported with inherent Ruthenium (Ru) sites where the framework controls reactant diffusion by suppressing proton supply and enhancing N_2 flux, causing highly selective and efficient catalysis. The smart catalyst design results in a remarkable ammonia production yield rate of 2.03 mg h^{-1} mg_{cat}^{-1} with an excellent F.E. of ≈52.9%. The findings are further endorsed with the

	help of molecular dynamics simulations and control COF systems without in situ proton filter feasibility. The results point to a paradigm shift in engineering high-performance NRR electrocatalysts for more feasible green NH_3 production.
11.	Analysis and mitigation of circulating common-mode current in isolated dual active bridge converter **B Dwiza, J Kalaiselvi** - 49th Annual Conference of the IEEE Industrial Electronics Society, 2023 **Abstract:** This paper deals with the phenomenon of the circulating current that propagates between the two H-Bridges via the ground, termed the circulating common-mode current (CCMC). The circumstances that facilitate the CCMC are presented with experimental validations. The propagation path and the voltage source of the CCMC are analyzed with the help of the commonmode (CM) equivalent circuit. In addition, the design of the coupled inductor to address the CCMC is discussed in detail. All the experimental validations are performed on a prototype DAB converter.
12.	Analysis of trip frequency choice of commute trips in the context of COVID-19 in India: A hybrid choice modelling approach with generalized ordered logit kernel **Bh Aaditya, TM Rahul** - IATSS Research, 2023 **Abstract:** The paradigm shift in mobility and travel behaviour caused by the successive waves of the COVID-19 pandemic has been unreal. The long-term effects of the pandemic resulting from the fear of the spread of the virus against the belief in the remedial measures are to be understood from a behavioural perspective to strengthen the current transportation system against such impediments. The current study adds to the literature on COVID-19 pandemic by unravelling the long-term impacts of the pandemic on the trip frequency of commute trips. A dataset of 467 individuals from all over India is analysed to understand the factors impacting the willingness of the respondents to reduce their commute trips in a post-vaccinated scenario. An integrated choice and latent variable structure, with a generalized ordered logit kernel, was considered to incorporate the influence of psycho-attitudinal variables and socio-demographics on the willingness to reduce trip frequency among individuals. The results indicate a significant impact for variables including fear of the virus spread, age of individuals, and job satisfaction of working from home on the stated willingness towards trip reduction. The study concludes by presenting policy measures that target to overcome the effects of the pandemic and restore normalcy. © 2023
13.	Analyzing managerial and technological barriers to the adoption of industry 4.0: An 'ISM' and 'MICMAC' approach **C Dixit, R Kumar** - IEEE Transactions on Engineering Management, 2023 **Abstract:** The aim of study is to identify the barriers that affect the implementation of Industry 4.0, establish the relationship among the barriers using interpretive structural modelling (ISM), and identify the driving power and dependence of the identified barriers using MICMAC analysis. Industry 4.0, a different acronym for the fourth industrial revolution, is considered an important concept for the digitalisation of the manufacturing sector as it results in the efficient use of resources, reduced lead time, and improved product quality. A contextual relationship matrix was constructed based on questionnaire responses from industry and academia. Then, hierarchical relationship among the identified barriers were established using ISM method. Subsequently, driving power and dependence of the identified barriers were identified using MICMAC analysis. The analysed results helped determine the significance of the identified barriers and their relative importance, which will in turn help researchers and policymakers in the implementation of the Industry 4.0 concept. This study also suggests that the government should frame the policy to provide financial and technical support and subsidies for transforming conventional factories into smart factories, and proper training should be given to the workforce

	so that they can cope with the real-time needs of the industries.
14.	Anisotropic properties of two-dimensional (2D) tin dihalide (SnX_2, X = Cl, Br, I) monolayer binary materials V Kumar, H Jeon… **R Ahuja**… - Journal of Physics: Condensed Matter, 2023 **Abstract:** This paper investigated the electronic properties and photoresponse of two-dimensional SnX_2 (X = Cl, Br, I) monolayer binary materials using computational techniques. The calculated band structure and density of states indicate that these are large band gap semiconducting materials with an indirect band gap. The studied chemical bonding mechanism shows the existence of the hybrid bonding of ionic and covalent bonds in these dihalide materials. The valence band (VB) and conduction band (CB) edge positions are also estimated, using the concept of electronegativity and band gap, to investigate the photocatalytic activity of SnX_2. Next, we investigated the polarization and energy-dependent dielectric and optical functions along the crystallographic axes of these materials in the linear response approach of the perturbing incident oscillating light field. These materials exhibit an anisotropic behavior of these functions, especially in the high-energy visible and low-energy ultraviolet (UV) regions. The absorption of incident light photons is very fast in SnI_2 than $SnBr_2$ and $SnCl_2$ in the low-energy UV region. It demonstrates the higher absorption coefficient and optical conductivity in SnI_2. The obtained average static refractive index of $SnCl_2$ is comparable to that of glass (1.5), showing its application as transparent material. The low reflection coefficient, less than 20%, makes them superior for antireflection coating materials in the infrared and visible regions. The prominent energy loss peaks show the existence of plasmon resonances in these materials. The most of losses occur in the UV region. The investigated electronic and photoresponse properties indicate that these Sn-based dihalide materials are excellent for electronic devices and optoelectronic applications. Also, the calculated VB and CB edge positions with respect to the normal hydrogen electrode show the favorable water-splitting capability of these materials.
15.	Background estimation studies for positron double Beta decay **S Thakur**…**PP Singh, PK Raina, RG Pillay** - WOMEN IN PHYSICS: 7th IUPAP International Conference on Women in Physics, 2023 **Abstract:** The study of neutrinoless double beta decay (DBD) has attracted much attention because it can provide valuable information about the mass and the nature of the neutrino. DBD itself is also of interest in nuclear physics. While DBD has been observed in about a dozen nuclei, the positron DBD ($\beta^+\beta^+$/EC-β+) continues to be elusive. An important signature for $\beta+\beta+$ decay is the simultaneous emission of four 511 keV gamma rays, and the coincident detection of these gamma rays can improve the measurement sensitivity. This paper presents an estimation of sensitivity for EC-β+and $\beta+\beta^+$, employing coincidence measurement with two high-purity Ge (HPGe) detectors. Simulations for coincident detection efficiency (εc) of 511 keV gamma rays with two HPGe detectors were carried out using GEANT4 for different source geometries to optimize the mass efficiency product (Mεc). A source of size 55 mm × 55 mm × 5 mm (thickness) sandwiched between the front faces of the detectors was found to be optimal for two pairs of 511 keV gamma rays in the present detector setup. The coincident background was estimated at sea level with moderate lead shielding. With this setup, the sensitivity for $T_{1/2}$ measurement of EC-β+in ^{112}Sn and $\beta+\beta^+$ in ^{106}Cd was estimated to be $\sim 10^{19}$–10^{20} years for one year of measurement time
16.	Basis set superposition error: effects of the boys–bernardi correction on the DFT modeling of hydrogen sorption on low-dimensional carbon nanomaterials KV Alantev, DV Babailova…**R Ahuja** - Bulletin of the Russian Academy of Sciences: Physics, 2023 **Abstract:** DFT modeling of hydrogen sorption on graphene and C2N monolayers using the SIESTA and VASP packages demonstrates the need for optimizing the pseudo-atomic orbital

	basis set and calculating the counterpoise correction to the basis set superposition error for H2 binding energy. The use of pseudo-atomic orbitals reduces the H2-monolayer distance by 10%, relative to plane wave data. The optimized pseudo-atomic orbital parameters for a C2N monolayer can be used to further investigate this material.
17.	Biodiversity Sensor: A Customized and Power Efficient Solution for Biodiversity Surveillance **M Kaur, K Singh, S Kumar** - IEEE Sensors Journal, 2023 **Abstract:** Pollinators play a vital role in ecosystem conservation, and their extinction would pose a serious threat to our existence. Recent research has revealed that excessive use of pesticides, fertilizers, and changing farming practices has adversely affected pollinator biodiversity. Therefore, continuous farmland monitoring is required to check flying insects for biodiversity conservation. The idea is to develop a digital sensor network across farmlands for the monitoring of biodiversity at a large scale. In this article, a biodiversity sensor (BS) is developed that can track the movement of flying insects in real-time, along with environmental conditions and updates to the cloud server. The developed sensor is a processor-based Internet of Things (IoT) device, powered by a solar photovoltaic (PV)/battery bank and loaded with a customized Linux operating system (OS) (using Yocto-build). An over-the-air (OTA) update feature has been added to the customized OS, allowing remote management and sensor updates that were previously unavailable in the pre-installed multimedia OS. The sensor can also be managed locally using the device manager portal (DMP), which exposes sensor configuration and data download features over a local Wi-Fi hotspot. The developed sensor has been tested in the field, and the result shows that the BS effectively captures the frames of flying insects and performs surveillance appropriately with an accuracy of more than 90%. A comparison of power efficiency and central processing unit (CPU) utilization is also made between the pre-installed multimedia OS from the manufacturer and the customized OS built using Yocto-build. Results demonstrate that the developed BS is power efficient.
18.	Biomedical applications of biogenic carbon-based fluorescent nanoparticles **K Kaur**, G Singh…**N Singh** - Biogenic Nanomaterial for Health and Environment: Book Chapter, 2023 **Abstract:** The wide-ranging applications of carbon dots (CDs), which can be developed using either green or chemical precursors, have been made possible due to their reported properties and the various precursors that have been identified. This has opened up new opportunities for the development of high-quality CDs and their use in optoelectronic devices, bioimaging, and other applications. Green precursors can be derived from fruits, vegetables, flowers, leaves, seeds, stems, crop residues, fungi/bacteria species, and waste products, while chemical precursors can be categorized as either acid reagents or non-acid reagents. It provides a brief review of the past ten years of CD synthesis using both green and chemical precursors, as well as the use of CDs as sensing materials in biomedical applications. This comprehensive review will be a valuable resource for researchers who are interested in synthesizing high-quality CDs for a variety of applications.
19.	Building supply chain resilience in developing economies: A weighted Ishikawa diagram approach A Patidar, M Sharma…**P Sarkar** - Operations Management Research, 2023 **Abstract:** This study aimed to identify the cause-and-effect relationship among the factors influencing a resilient supply chain and to quantify their importance using a cause and effect (Ishikawa) diagram and Multi-Criteria Decision Making (MCDM) tool respectively. The results showed that redesigning the network and creating a supply chain buffer were the most important criteria/pillars, and the most important factors were creating redundancy and robustness. The study also found that approximately 80% and 20% of resilience can be achieved by developing

	absorption and reactive capabilities, respectively. The importance weight provided by this study can be used by industry professionals to estimate achieving supply chain resilience, while academicians can use it as the foundation for future researches. Further, researches may be carried out by developing a digital twin to understand potential impact of disruptions and resilience strategies. Blockchain implementation precisely smart contracts may be studied, since it appears to be one among best solutions to create transparency, coordination and control mechanism in the supply chain system. The novelty of this study lies in the weighted Ishikawa diagram that quantifies the contribution of each factor in percentage terms, providing specific insights into the factors influencing supply chain resilience.
20.	Capturing Sialyl-glycan on live cancer cells by tailored boronopeptide **S Chatterjee, A Chowdhury, S Saproo, NM Tripathi… S Naidu, A Bandyopadhyay** - Chemistry- A European Journal, 2023 **Abstract:** Boronic acid-containing molecules are substantially popularized in chemical biology and medicinal chemistry due to the broad spectrum of covalent conjugations as well as interaction modules offered by the versatile boron atom. Apparently, the WGA peptide (wheat germ agglutinin, 62–73), which shows a considerably low binding affinity to sialic acid, turned into a selective and >5 folds potent binder with the aid of a suitable boronic acid probe installed chemoselectively. In silico studies prompted us to install BA probes on the cysteine residue, supposedly located in close proximity to the bound sialic acid. In vitro studies revealed that the tailored boronopeptides show enhanced binding ability due to the synergistic recognition governed by selective non-covalent interactions and cis-diol boronic acid conjugation. The intense binding is observed even in 10 % serum, thus enabling profiling of sialyl-glycan on cancer cells, as compared with the widely used lectin, Sambucus nigra. The synergistic binding mode between the best boronopeptide (P3) binder and sialic acid was analyzed via 1H and 11B NMR. 
21.	Chaotropic anion induced self-assembly of naphthalimide–glutathione nanohybrids: selective recognition of bisulphate anions in aqueous medium **A Singh**, M Chaudhary, **M Verma**…**N Singh** - New Journal of Chemistry, 2023 **Abstract:** Anion-induced self-assembly is one of the growing research fields as it provides a better understanding of natural self-assemblies such as DNA, proteins, peptides, *etc*. Peptides are well known for their aggregation properties owing to their hydrogen bonding interactions. Herein, nanohybrids of the glutathione tripeptide and naphthalimide based compounds were fabricated, in order to explore their self-assembly behaviour. The naphthalimide based compounds were processed into organic nanoparticles using a re-precipitation method and then into nanohybrids with a tripeptide under ultrasonication conditions to get nanohybrids NH-1, NH-2 and NH-3. The morphology of prepared nanohybrids was studied by HRTEM analysis. The photophysical studies of these nanohybrids were carried out by adding various anions. NH-1 shows enhanced fluorescence intensity with bisulphate anions and the rest of the anions do not induce any change in the fluorescence intensity. Furthermore, the morphology of these nanohybrids was monitored using HRTEM and STEM. With bisulphate anions, a beautiful butterfly shaped self-assembly was observed for NH-1. The increase in intensity was a result of

	the aggregation induced enhanced emission mechanism. These self-assemblies have potential applications in the recognition of bisulphate with a limit of detection (LOD) of 3 nM and a limit of quantification of 10 nM respectively.
22.	Chasing the intruder: a reinforcement learning approach for tracking unidentified drones **S Kainth, S Sahoo, R Tilak, SS Jha** - AIR '23: Proceedings of the 2023 6th International Conference on Advances in Robotics, 2023 **Abstract:** Drones are becoming versatile in a myriad of applications. This has led to the use of drones for spying and intruding into the restricted or private air spaces. Such foul use of drone technology is dangerous for the safety and security of many critical infrastructures. In addition, due to the varied low-cost design and agility of the drones, it is a challenging task to identify and track them using the conventional radar systems. In this paper, we propose a reinforcement learning based approach for identifying and tracking any intruder drone using a chaser drone. Our proposed solution uses computer vision techniques interleaved with the policy learning framework of reinforcement learning to learn a control policy for chasing the intruder drone. The whole system has been implemented using ROS and Gazebo along with the Ardupilot based flight controller. The results show that the reinforcement learning based policy converges to identify and track the intruder drone. Further, the learnt policy is robust with respect to the change in speed or orientation of the intruder drone.
23.	Climate uncertainty and vulnerability of urban flooding associated with regional risk using multi-criteria analysis in Mumbai, India Y Nilesh, Wu, Jianping, B Abhishek, **P Shray** ...- Environmental Research, 2024 **Abstract:** The study made a comprehensive effort to examine climatic uncertainties at both yearly and monthly scales, along with mapping flood risks based on different land use categories. Recent studies have progressively been engrossed in demonstrating regional climate variations and associated flood probability to maintain the geo-ecological balance at micro to macro-regions. To carry out this investigation, various historical remote sensing record, reanalyzed and in-situ data sets were acquired with a high level of spatial precision using the Google Earth Engine (GEE) web-based remote sensing platform. Non-parametric techniques and multi-layer integration methods were then employed to illustrate the fluctuations in climate factors alongside creating maps indicating the susceptibility to floods. The study reveals an increased pattern in LST (Land Surface Temperature) (0.03 °C/year), albeit marginal declined in southern coastal regions (−0.15 °C/year) along with uneven rainfall patterns (1.42 mm/year). Moreover, long-term LULC change estimation divulges increased trends of urbanization (16.4 km2/year) together with vegetation growth (8.7 km2/year) from 2002 to 2022. Furthermore, this inquiry involves numerous environmental factors that influence the situation (elevation data, topographic wetness index, drainage density, proximity to water bodies, slope, and soil properties) as well as socio-economic attributes (population) to assess flood risk areas through the utilization of Analytical Hierarchy Process and overlay methods with assigned weights. The outcomes reveal nearly 55 percent of urban land is susceptible to flood in 2022, which were 45 and 37 percent in 2012 and 2002 separately. Additionally, 106 km2 of urban area is highly susceptible to inundation, whereas vegetation also occupies a significant proportion (52 km2). This thorough exploration offers a significant chance to formulate flood management and mitigation strategies tailored to specific regions during the era of climate change. © 2023 Elsevier Inc.
24.	Comparative study of surface integrity for AZ31B magnesium alloy during the application of ultrasonic vibration and laser energies in the turning process **N Deswal, R Kant** - Journal of Materials Engineering and Performance, 2023 **Abstract:** AZ31B magnesium alloys are significant materials for biomedical, aviation, and automotive industries. But, the poor surface properties of AZ31B magnesium alloys limit their

	usage for wider applications. Literature suggests that hybrid machining processes have achieved better machining performance compared to the conventional turning (CT) process without using any cutting fluids. Therefore, an attempt has been made to improve the surface integrity of AZ31B magnesium alloy in terms of machining forces, machining temperature, chip morphology, surface roughness, surface damage, microstructure, microhardness, residual stresses, and corrosion behavior during a recently developed hybrid machining technology, i.e., ultrasonic-vibration-laser-assisted turning (UVLAT). A comparative surface integrity analysis has been carried out among the CT, ultrasonic vibration-assisted turning (UVAT), laser-assisted turning (LAT), and UVLAT processes. The results of the current study indicate significant benefits of the UVLAT process on surface integrity. Machining forces and surface roughness were reduced by 42-61% and 18-33%, respectively, for the UVLAT process than the other processes. However, the machining temperature was increased by 8-83% during the UVLAT process compared to the other processes. Ductile chips, smooth surface, and higher grain refinement were obtained in the UVLAT process when compared with other processes. Residual stresses were found more compressive in nature for the UVLAT process than that of the other processes. Microhardness and corrosion resistance were increased by 28-106% and 13-56%, respectively, during the UVLAT process in comparison with the other processes. This might be ascribed to the frequent tool separation and workpiece material thermal softening, simultaneously. The UVLAT process can be beneficial for diverse applications due to the improvement in surface properties.
25.	Control of spectral properties in 1d defective photonic crystals by doping with two-level atoms **N Ghangas, S Dasgupta** - Laser Science, 2023 **Abstract:** We investigated the spectral properties in one dimensional defective photonic crystals by doping defect layer with the two-level atoms and observed the switching of near-complete reflection to zero in the critical coupling regime.
26.	Corrosion behaviour of plasma-sprayed baghdadite bioceramic coatings reinforced with carbon nanotubes S Singh, A Kumar…**B Das , K Rakha , H Singh** - Journal of Alloys and Compounds, 2023 **Abstract:** Bioceramics have been extensively used for the restoration and replacement of hard tissues, such as bones and teeth due to their physicochemical resemblance to these tissues. This study focuses on enhancing the properties of plasma-sprayed bioceramic coatings with the addition of carbon nanotubes. The coatings deposited include hydroxyapatite, baghdadite, and baghdadite with carbon nanotube reinforcement. The effect of incorporating carbon nanotubes into baghdadite coatings is thoroughly investigated in terms of microstructural, mechanical, and electrochemical properties. Multiple characterization techniques such as scanning electron microscopy, energy dispersive spectroscopy, X-ray diffractometry, and Raman spectroscopy have been employed to reveal microstructural details, elemental composition, and phase constituents of the deposited coatings. The results indicate that baghdadite coatings exhibit higher porosity compared to hydroxyapatite coatings. However, the addition of carbon nanotubes as reinforcement into baghdadite coatings effectively reduces porosity by integrating carbon nanotubes within the inter-lamellae structure and filling voids within the inter-splat regions. This integration also mitigates common post plasma spray defects including porosity, voids, and microcracks. The incorporation of 2 wt% carbon nanotubes into the baghdadite matrix results in a substantial 80% reduction in corrosion current density(Icorr). This reduction is attributed to the combined effects of reduced porosity, and improved structural integrity due to carbon nanotubes. Furthermore, the carbon nanotubes reinforced baghdadite coatings have indicated the healthy development of the MC3T3-E1 osteoblast cell line.
27.	Creep crack growth characterization of SS316LN

	AK Mishra, A Gopalan… **A Tiwari** - Materials at High Temperatures, 2023 **Abstract:** In creep conditions, conventionally, C* and C(t) line integrals are used for characterising the crack tip. However, the true crack driving force or its rate cannot be described by any of the conventional parameters. The theoretical validity of conventional crack tip-characterising parameters like J or Ct is also restricted, making it hard to anticipate the driving forces underlying cracks. To investigate the creep crack growth behaviour of this material an experimental analysis of SS316LN at 650 °C is performed. The crack extension is modelled through the node-release technique, and a configurational force-based rate of change of J integral is calculated by post-processing of the finite element results. The results show that the Ct and dJepc/dt calculated from FE analyses are similar and the trend is also similar to the experimentally measured C*-values.
28.	Criteria for close-to-convexity, convex in one direction of planar harmonic mappings **K Jaglan, AS Kaliraj** - The Journal of Analysis, 2023 **Abstract:** In this article, we prove sufficient conditions for a normalized complex-valued harmonic function f defined on the unit disk to be univalent and convex in one direction/close-to-convex. Using the geometric properties of convex in one direction or close-to-convex function, we obtain sufficient conditions for univalency in terms of certain integral inequalities. With the help of an integral inequality, we prove a sharp coefficient criteria for f to be convex in one direction. As an application, we finally generate families of univalent harmonic mappings convex in one direction using Gaussian hypergeometric functions.
29.	Detecting meso-damage and subsurface cracks in a hard rock using frequency-modulated thermal wave imaging (FMTWI) **M Jaiswal, R Sebastian**, R Mulaveesala - Measurement Science and Technology, 2023 **Abstract:** Mines, tunnels, and hillside roadways that are subjected to high levels of stress are prone to massive and violent occurrences of rock failures. It results in a multitude of irreversible consequences, including the loss of human lives. Nevertheless, preceding rock failures, the development of micro and macrocracks, which are sometimes not discernible on the surface, takes place. Subsurface cracks indicate the degradation of rock and can be employed as a means to anticipate occurrences of rock failures and bursts. Therefore, the utilization of subsurface imaging techniques for rocks facilitates the estimation of the true strength of the rock mass. Nevertheless, in many instances, rock masses are not easily reachable, posing difficulties for standard techniques such as ground-penetrating radar or computed tomography (CT) scan imaging, to identify the cracks. Hence, this research endeavours to explore the feasibility of employing frequency-modulated thermal wave imaging (FMTWI) for identifying subsurface cracks and their coalescence in hard rocks through the utilization of numerical simulation and experimental methods. A model was constructed using the finite element method wherein artificial cracks were intentionally introduced into a cylindrical granite specimen based on the CT scan data acquired during the meso-damage analysis. The thermograms obtained were subjected to pre-processing and post-processing techniques, and afterwards compared with the CT scan images. The FMTWI tests were conducted in the laboratory to calibrate and validate the simulation results. The findings derived from the analyses of temperature profiles and thermograms indicate that this particular technology is a promising one and offers several advantages in comparison to alternative methods for detecting micro- or macrocracks in deep mines and tunnels.
30.	Development of a low-cost, compact, wireless, 16 - channel biopotential data acquisition, signal conditioning and arbitrary waveform stimulator **RS Halder, B Basumatary, A Sahani** - Biomedical Physics & Engineering Express, 2023

	Abstract: The health and fitness of the human body rely heavily on physiological parameters. These parameters can be measured using various tools such as ECG, EMG, EEG, EOG, among others, to obtain real-time physiological data. Analysing the bio-signals obtained from these measurements can provide valuable information that can be used to improve health-care in terms of observation, diagnosis, and treatment. In bio-signal pattern recognition applications, more channels provide multiple information simultaneously. Different biosignal acquisition devices are available in the market, most of which are designed for specific signals like ECG, EMG, EEG etc. The gain of the amplifiers and frequency of the filters are designed as per the targeted signals; due to which one device cannot be used for other signals. Also, most of the systems are wired system which is not comfortable for animal studies. In this paper, a low-cost, compact, wireless, 16 channel biopotential data acquisition system with integrated electrical stimulator is designed and implemented. There are several novel and flexible design approaches were incorporated in the proposed design like (1) It has user selectable digital filter in each channel based on the signal frequencies like ECG, EMG, EEG, EOG. The same system will be used to acquire different signals simultaneously. (2) It has variable gain with configurable analog bandpass filter. (3) It can acquire signals from 4 patients simultaneously. (4) The system is capable to acquire signal from both two-electrode as well as three-electrode configurations. (5) It has integrated stimulator with trapezoidal, charge-balanced, biphasic stimulus output with near zero DC level and user selectable pulse duration or frequency of the stimulus. The developed system has the ability to acquire and transmit data wirelessly in real-time at a high transfer rate. To validate the performance of the system, tests were conducted on the acquired signals using a simulator.
31.	Dynamics of thin self-rewetting liquid films on an inclined heated substrate **M Zubair, R Vellingiri** - Journal of applied physics, 2023 **Abstract:** In this paper, we investigate the quadratic Marangoni instability along with inertia in a self-rewetting fluid film that has a nonmonotonic variation of surface tension with temperature. The dynamics of such a thin self-rewetting fluid film flowing along an inclined heated substrate is examined by deriving an evolution equation for the film thickness using long-wave theory and asymptotic expansions. By adopting the derived long-wave model that includes the inertial and thermocapillary effects, we perform a linear stability analysis of the flat film solution. Two cases of the nonlinear flow are explored in depth using T_m (temperature corresponding to the minimum of surface tension) as the cutoff point. One is the case of $(T_{i+s} - T_m)<0$, and the other is $(T_{i+s} - T_m)>0$, where T_{i+s} is the interface temperature corresponding to the flat film. The Marangoni effect switches to the anomalous Marangoni effect as $(T_{i+s} - T_m)$shifts from a negative value to a positive value. Our calculations reveal that the Marangoni effect augments the flat film instability when $(T_{i+s} - T_m)<0$, whereas the stability of the flat film is promoted for $(T_{i+s} - T_m)>0$. Our further analysis demonstrates that the destabilizing inertial forces can be entirely compensated by the stabilizing anomalous thermocapillary forces. We verify the linear stability predictions of the long-wave Benney-type model with the solution to the Orr–Sommerfeld problem in the long-wave limit. Our time-dependent computations of the long-wave model establish the modulation of interface deformation in the presence of inertia and temperature gradients in the conventional Marangoni regime, whereas such deformations are suppressed in the anomalous Marangoni regime. A comparison of the numerical computations with the linear theory shows good agreement.
32.	Early warning signals have limited applicability to empirical lake data DA O'Brien, **S Deb**… **PS Dutta** … - Nature Communications, 2023 **Abstract:** Research aimed at identifying indicators of persistent abrupt shifts in ecological communities, a.k.a regime shifts, has led to the development of a suite of early warning signals (EWSs). As these often perform inaccurately when applied to real-world observational data, it remains unclear whether critical transitions are the dominant mechanism of regime shifts and, if

	so, which EWS methods can predict them. Here, using multi-trophic planktonic data on multiple lakes from around the world, we classify both lake dynamics and the reliability of classic and second generation EWSs methods to predict whole-ecosystem change. We find few instances of critical transitions, with different trophic levels often expressing different forms of abrupt change. The ability to predict this change is highly processing dependant, with most indicators not performing better than chance, multivariate EWSs being weakly superior to univariate, and a recent machine learning model performing poorly. Our results suggest that predictive ecology should start to move away from the concept of critical transitions, developing methods suitable for predicting resilience loss not limited to the strict bounds of bifurcation theory.
33.	Effect of compressed air cooling on tool wear during ultrasonic-vibration-laser assisted turning of aluminium alloy **N Deswal, R Kant** - Journal of Vibration Engineering & Technologies, 2023 **Abstract:** The utilization of various energy sources to assist the machining process has become prominent to achieve substantial improvement in machining performance. These energy sources have also resulted in an alternative to cutting fluids which is safer for both the universe and human beings. The combined action of laser and ultrasonic vibration energies during the turning process has shown significant achievement in machining process capabilities. Moreover, the application of higher compressed air pressure has achieved substantial improvement in machinability during the turning process.
34.	Effect of Electrometer Internal Circuit Parameters in Interpretation of Conduction Current Transient Characteristics **C Iyyappan, CC Reddy** - Proceedings of the International Symposium on Electrical Insulating Materials, 2023 **Abstract:** Conduction current measurements of insulating materials have traditionally relied on commercial electrometers as the primary equipment. Previous studies have documented diverse current dynamics exhibited by polymer insulating materials when subjected to different voltage and temperature conditions. These current characteristics are closely related to the charge dynamics of the polymers. However, little attention has been given to exploring potential instrumental errors associated with these measurements. In this study, authors address this gap by conducting circuit simulations using a linear equivalent circuit model of dielectrics. The simulations incorporate the internal circuitry of commercial electrometers. The current and voltage characteristics of the measuring circuit and polymers were discussed. Furthermore, performed experiments to replicate the electrometer setup and observed and reported variations in the conduction current characteristics that occur with changes in the internal circuit parameters.
35.	Effect of Hf and Al on self-diffusion in amorphous silica using molecular dynamics **Jhalak,** G Balasubramanian, **PK Ray** - JOM, 2023 **Abstract:** Mo-Si-B alloys and ultra-high-temperature ceramics including ZrB_2-based ceramics are potential candidates for hypersonic applications. In Mo-Si-B base systems and with SiC addition to ZrB_2, a protective SiO_2 rich glassy scale is formed at the surface. Diffusion through the scale and scale viscosity play an important role in understanding the oxidation behavior of the system. In the present work, the diffusion coefficient and activation energies of the diffusing species have been calculated using molecular dynamics, as these govern the scale growth and surface coverage. The effects of Hf and Al additions to the SiO_2 have also been studied. Si^{4+} ions substitution with Hf^{4+} was found to increase the activation energy of both Si^{4+} and O^{2-} ions with the increase in their concentration. On the other hand, Al^{3+} ions reduced the activation energy with a reversal in trend at higher content. However, in both cases, the diffusivity values of the added cations were highest and that of Si^{4+} ions were lowest

36.	Efficient virtual impedance-based active damping for LCL filter resonance in grid connected inverter using inverter and grid current as feedback **G Teotia, AV Ravi Teja** - 49th Annual Conference of Industrial Electronics Society, 2023 **Abstract:** LCL filter resonance complicates the design of a current control loop, threatens its stability, and increases harmonic content in output current at the resonance frequency. This paper presents a novel active damping approach based on the virtual resistor. The proposed method utilize the inverter side current and grid side current as feedback variable to provide the virtual effect of three different damping resistors. The derived feedback gains are free from frequency terms and so do not contain any differential and integral terms which makes their implementation easy, requires less computation, and avoids noise amplification in the current control loop. Importantly, this method does not require any extra voltage/current sensor, the sensor already in use for current controlling and protection purposes is utilized for the implementation of the proposed active damping. Finally, the proposed method is simulated using MATLAB/Simulink and the simulation result justify the effectiveness of the proposed method.
37.	Electrochemical 1, 3-oxofluorination of gem-difluoro cyclopropanes: approach to α-cf3-substituted carbonyl compounds **S Dutt, R Kumar, N Banerjee, D Saha, P Banerjee** - Advanced Synthesis & Catalysis, 2023 **Abstract:** An electrochemicalmethodologyfor theconstructionofα-CF3-substitutedcarbonylcom-poundsin moderateto good yields under exogenousmetal and oxidant-freeconditionshas been devel-oped.The protocolinvolvesthe single-electronoxidationof the aryl ring to generatea radicalcationfollowedby a three-electronSN2 reactionresultingin the formationofα-CF3substitutedketones. 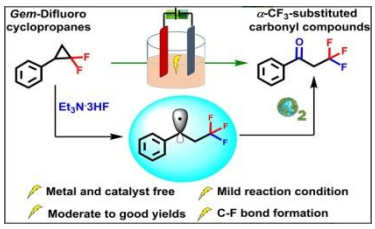
38.	Exclusion processes on a roundabout traffic model with constrained resources **A Gupta, A K Gupta** - Physical Review E, 2023 **Abstract:** Motivated by the vehicular traffic phenomenon at roundabouts, we examine how the limited availability of resources affects the movement of two distinct types of particles on bidirectional lanes connected by two bridges, with each bridge specifically designated for the transportation of one species. To provide a theoretical ground for our findings, we employ a mean-field framework and successfully validate them through dynamic Monte Carlo simulations. Based on the theoretical analysis, we analytically derive various stationary properties, such as the particle densities, phase boundaries, and particle currents, for all the possible symmetric as well as asymmetric phases. The qualitative as well as quantitative behavior of the system is significantly affected by the constraint on the number of resources. The complexity of the phase diagram shows a nonmonotonic behavior with an increasing number of particles in the system. Analytical arguments enable the identification of several critical values for the total number of particles, leading to a qualitative change in the phase diagrams. The interplay of the finite resources and the bidirectional transport yields unanticipated and unusual features such as back-and-forth transition, the presence of two congested phases where particle movement is halted, as well as shock phases induced by boundaries and the bulk of the system. Also, it is found that spontaneous symmetry-breaking phenomena are induced even for very few particles in the system. Moreover, we thoroughly examine the location of shocks by varying the parameters

	controlling the system's boundaries, providing insights into possible phase transitions.
39.	Explicit k-means clustering assisted direct model for identification of groundwater pollution sources J Chaubey, **D Kashyap** - Environmental Forensics, 2023 **Abstract:** A computationally inexpensive and data parsimonious direct model for identification of groundwater pollution sources that captures their location, spatial extent and flux intensities at a chosen reference time is presented in this study. The model is based upon instantaneous micro-level mass balance that is depicted by a pseudo steady state solute transport equation. Clusters of polluting locations were identified by finite differencing the solute transport equation and applying K-means clustering algorithm. The model is validated by the problem taken from Singh, Datta, and Jain (Citation2004) and is also illustrated by applying it to an area lying between river Krishni and Hindon. Validation results showed that the model captured closely the pollution source locations; their corresponding spatial extents and flux intensities. Model captured the sources even when the concentration plumes are far away from the source locations due to advection dominated contaminant transport. Illustration results showed that the model identified the leachate flux intensity from irrigation in the form of a regional source. Further, it established a few local sources arising possibly out of localized industrial and/or municipal waste water disposal.
40.	Fusion and decay dynamics of and reactions across the Coulomb barrier N Grover, I Sharma … **PK Raina** - Physical Review C, 2023 **Abstract:** In reference to the complete fusion (CF) and incomplete fusion (ICF) processes, the analysis of 6Li+120Sn and 7Li+119Sn reactions forming the 126I compound nucleus (CN) is carried out at incident energies spreading across the Coulomb barrier. The theoretical calculations of the formation of the compound nucleus 126I via two different entrance channels are done by opting for the energy-dependent Woods-Saxon potential (EDWSP) model and the ℓ-summed Wong model. The available CF cross-section data of these systems at above-barrier energies is suppressed with respect to the EDWSP outcomes, and a reducing factor is needed to explain above-barrier CF data of given reactions. Such suppression effects at above-barrier energies can be correlated with the breakup of weakly bound systems (6,7Li) before reaching the Coulomb barrier. The total fusion (TF) cross-section data, which are the sum of CF and ICF cross-section data, are fairly addressed by using the EDWSP predictions. The difference between CF and TF data represents ICF yields and hence qualified in terms of range parameter r0. Besides this, the ℓ-summed Wong approach has been used to address CF, ICF, and TF cross-section data, which limits the contribution of partial waves to the maximum ℓ value. Within the ℓ-summed Wong model, the CF and ICF contributions are separated out on the basis of the angular-momentum window. In the angular-momentum distribution case, CF and ICF contributions are estimated in view of ℓ-windows assigned for CF (ℓ=0 to ℓcrit.) and ICF (ℓcrit. to ℓmax) components. Furthermore, the decay analysis of 126I compound nucleus is made using the dynamical cluster decay model (DCM). Calculations are made to analyze the decay cross sections σxn of neutron channels for given entrance channels at a wide spread of energies (Elab=14–28 MeV). The neck-length parameter ΔR, which decides the first turning point, is optimized to address the decay cross sections of different neutron evaporation channels and DCM-based calculations fairly explained the decay patterns of the CN.
41.	Groundwater quality index development using the ANN model of Delhi Metropolitan City, India A Gani, M Singh, **S Pathak**, A Hussain - Environmental Science and Pollution Research, 2023 **Abstract:** Groundwater is widely recognized as a vital source of fresh drinking water worldwide. However, the rapid, unregulated population growth and increased industrialization, coupled with

	a rise in human activities, have significantly harmed the quality of groundwater. Changes in the local topography and drainage systems in an area have negative impacts on both the quality and quantity of groundwater. This underscores the critical need to assess the susceptibility of groundwater to pollution and implement measures to mitigate these risks. The water quality index (WQI) is an approach that simulates the water quality at peculiar locations for a particular period of time. The artificial neural network (ANN) model approach is such an idealistic methodology that can be utilized for WQI development and provides better results for specific locations in optimum time. Therefore, the goal of the current study is to provide a unique way for using artificial neural networks (ANN) to characterize the groundwater quality of Delhi Metropolitan City, India. In order to make the water fit for residential and drinking use, the research also pinpoints the geographical variability and spots where the contaminated region has to be sufficiently cleaned. A minimum WQI of 41.51 was obtained at the Jagatpur location while a maximum value of 779.01 was at the Peeragarhi location. During the training phase, the results obtained using the ANN model were highly favorable, demonstrating a strong association with an *R*-value of 98.10%, thus highlighting the program's exceptional efficiency. However, in accordance with the correlation regression findings, the prediction outcomes of the ANN model in testing are observed to be an *R*-value of 99.99–100%. This study confirms the promise and advantages of employing advanced artificial intelligence in managing groundwater quality in the studied area.
42.	Group and individual fairness in clustering algorithms **S Gupta, S Jain…**NC Krishnan, N Hemachandra - Ethics in Artificial Intelligence: Bias, Fairness and Beyond: Book Chapter, 2023 **Abstract;** Clustering is a classical unsupervised machine learning technique. It has various applications in criminal justice, automated resume processing, bank loan approvals, recommender systems, and many more. Despite being so popular, traditional clustering algorithms may result in discriminatory behavior towards a group of people (or individuals) and have societal impacts. It has led to the study of fair clustering algorithms that aim to minimize the clustering cost while ensuring fairness. This chapter outlines existing group and individual fairness notions, discusses their relationships, and comprehensively categorizes the current algorithms. The chapter further discusses the advantages and disadvantages of existing algorithms in terms of theoretical guarantees, time complexity, and reproducibility. Finally, the chapter concludes with a discussion of new directions and open problems in the field of fair clustering.
43.	HTree: hardware trojan attack on cache resizing policies **A Kumar, S Das, B Subba** - IEEE Embedded Systems Letters, 2023 **Abstract:** Modern Chipmultiprocessors (CMP) use third-party intellectual properties (IP) to reduce design costs and meet deadlines. The cores in the CMP has their own private cache memories and all the cores share a common large sized Last Level Cache (LLC). All the components of CMP including cores and cache memories are connected through a Network-on-Chip (NoC). Most of the NoC components have third-party IPs. Some of these IPs may be malicious and act as Hardware Trojan (HT). In this work, we propose an HT-base attack that targets the LLC resizing techniques. The LLC resizing techniques are used to reduce the energy consumption of the LLC by shutting down unused parts of the LLC. The proposed attack can misuse the properties of these resizing techniques to reduce their energy saving up to 58%. The proposed attack can also reduce the system performance up to 18%.
44.	Heat Transfer in Simultaneously Developing Turbulent Mixed Convection Flows in Vertical Tubes **S Gorai, D Samanta**, SK Das - Heat Transfer Engineering, 2023

	Abstract: This article investigates the simultaneously developing pure turbulent mixed convective regime and compares the hydrodynamic and thermal features of both buoyancy-assisted and opposed flows in a vertical tube. Two-dimensional (2D) axisymmetric steady-state simulations were carried out for Reynolds number, 5,000–20,000; Grashof number, 1.25 × 106 to 108; and Richardson number, 0.05–0.25 for a length-to-diameter ratio of 150 with uniform heat flux boundary condition and water as the working fluid. Three Reynolds-averaged-Navier–Stokes turbulence models were compared and then the most suitable model was used for the simulations. At a given Richardson number, the friction factor and Nusselt number are lower in the case of buoyancy-assisting flow compared to buoyancy-opposing flows. Similar friction factors and heat transfer trends were obtained at a given Grashof number. At varying Grashof numbers and Richardson numbers keeping the Reynolds number constant, no discernible variations were observed for both flows. The entry length was also examined, and it has been found that the hydrodynamic and thermal entry lengths are restricted to a length-to-diameter ratio of 25 and 20 for assisting and opposing flows, respectively. Correlations were developed for both flows to quantify the friction factor, Colburn factor, and Nusselt number in terms of the Reynolds number.
45.	Homogenization and corrector result of optimal control problem for Stokes system **R Raj, BC Sardar** - Complex Variables and Elliptic Equations,2023 **Abstract:** This article introduces the boundary optimal control problem in an N-dimensional domain governed by the stationary Stokes equations. Controls are applied to the states through Neumann data on the boundary. The aim of this paper is to study the asymptotic behavior of optimal control and states and identify the limit optimal control problem in the framework of the two-scale convergence. Finally, strong convergence of L2 -cost functional and a corrector result for velocities is proved.
46.	Identification, synthesis, and characterization of an unprecedented *N*-(2-carboxyethyl) adduct impurity in an injectable ganirelix formulation R Jadav, **R Kameriya, S Chatterjee, V Gour…A Bandyopadhyay** - Journal of Peptide Science, 2023 **Abstract:** Ganirelix, a peptide-based drug used to treat female infertility, has been in high market demand, which attracted generic formulation. A hitherto unknown impurity of ganirelix was observed in our formulation process, which reached ~0.3% in 6 months and led to a detailed investigation of its structure. In-depth analysis of ESI-MS/MS data of this impurity coupled with an artificial intelligence prediction tool led to a highly unusual putative structure, that is, N-(2-carboxyethyl)-ganirelix (^{N}CE-GA), which was authenticated by chemical synthesis from ganirelix and NMR analysis and via corroborated HPLC and MS/MS data with the formulation-derived impurity.
47.	In-silico analysis of optimal configurations for rotational bioinspired bone marrow biopsy needle designs: an ANN approach **R Nadda**, **R Repaka** - Annals of Biomedical Engineering, 2023 **Abstract:** Medical needle innovations have utilized rotating motion to enhance tissue-cutting capabilities, reducing cutting force and improving clinical outcomes. This study analyzes the effects of six essential factors on insertion and extraction forces during bone marrow biopsy (BMB) procedures. The study uses Taguchi's L32 orthogonal array and numerically simulates the BMB process using the Lagrangian surface-based method on a three-dimensional (3D) heterogeneous Finite Element (FE) model of the human iliac crest. The study evaluates cutting forces in needle insertion and extraction using uni-directional (360° rotation) and bidirectional (180° clock and anti-clock rotation) bioinspired BMB needles. This work aims to create an AI tool that assists researchers and clinicians in selecting the most suitable and safe design parameters for a bio-inspired barbed biopsy needle. An efficient Graphical User Interface (GUI)

	has been developed for easy use and seamless interaction with the AI tool. With a remarkable accuracy rate exceeding 98%, the tool's predictions hold significant value in facilitating the development of environmentally conscious biopsy needles. The tool demonstrates significantly higher efficiency compared to Abaqus, rendering it a valuable asset for researchers and clinicians engaged in bio-inspired biopsy needle development.
48.	In-situ synthesized polymer-derived sic reinforced aluminum matrix composites CV Girish, **H Singh, RM Prasad** - Journal of Alloys and Compounds, 2023 **Abstract:** In the current work, in-situ formed polymer-derived SiC reinforced aluminum-based metal matrix composites were synthesized to uniformly distribute ceramic particles in metal matrix with good matrix-reinforcement interface. Polymeric precursor (allyl hydrido polycarbosilane) was cross-linked at 300 °C and the cross-linked precursor was mixed with molten aluminum at 800 °C under nitrogen using stir casting route to obtained composites reinforced with 2 wt%, 4 wt% and 7 wt% of SiC (particle size < 10 μm) distributed uniformly in the synthesized composites. Structural characterization of samples were performed using FTIR, XRD, optical microscopy, FESEM and Raman spectroscopy. The composites demonstrated significant improvements in hardness (~58%), ultimate tensile strength (~45%) and compressive strength (~58%) for 7 wt% in-situ formed SiC in aluminum matrix compared to pure aluminum. 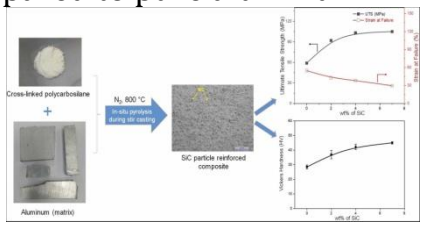
49.	Investigation of noise correlations in the phase-locked class-A VECSEL array S Karuseichyk, **V Pal,** S Sahoo… - Optics Express, 2023 **Abstract:** We theoretically and experimentally study the noise correlations in an array of lasers based on a VECSEL (Vertical External Cavity Surface Emitting Laser) architecture. The array of two or three lasers is created inside a planar degenerate cavity with a mask placed in a self-imaging position. Injection from each laser to its neighbors is created by diffraction, which creates a controllable complex coupling coefficient. The noise correlations between the different modes are observed to be dramatically different when the lasers are phase-locked or unlocked. These results are well explained by a rate equation model that takes into account the class-A dynamics of the lasers. This model permits the isolatation of the influence of the complex coupling coefficients and of the Henry α-factor on the noise behavior of the laser array.
50.	Leveraging different learning styles for improved knowledge distillation in biomedical imaging **U Niyaz, AS Sambyal, DR Bathula** - Computers in Biology and Medicine, 2023 **Abstract:** Learning style refers to a type of training mechanism adopted by an individual to gain new knowledge. As suggested by the VARK model, humans have different learning preferences, like Visual (V), Auditory (A), Read/Write (R), and Kinesthetic (K), for acquiring and effectively processing information. Our work endeavors to leverage this concept of knowledge diversification to improve the performance of model compression techniques like Knowledge Distillation (KD) and Mutual Learning (ML). Consequently, we use a single-teacher and two-student network in a unified framework that not only allows for the transfer of knowledge from teacher to students (KD) but also encourages collaborative learning between students (ML).

	Unlike the conventional approach, where the teacher shares the same knowledge in the form of predictions or feature representations with the student network, our proposed approach employs a more diversified strategy by training one student with predictions and the other with feature maps from the teacher. We further extend this knowledge diversification by facilitating the exchange of predictions and feature maps between the two student networks, enriching their learning experiences. We have conducted comprehensive experiments with three benchmark datasets for both classification and segmentation tasks using two different network architecture combinations. These experimental results demonstrate that knowledge diversification in a combined KD and ML framework outperforms conventional KD or ML techniques (with similar network configuration) that only use predictions with an average improvement of 2%. Furthermore, consistent improvement in performance across different tasks, with various network architectures, and over state-of-the-art techniques establishes the robustness and generalizability of the proposed model.
51.	Machine learning algorithm-based prediction of machined surface quality in end milling operation **J Airao, A Gupta, G Saraf, CK Nirala** - AIR '23: Proceedings of the 2023 6th International Conference on Advances in Robotics, 2023 **Abstract:** Machine learning (ML) has become an important tool for the development of Industry 4.0. It assists the machining processes by monitoring and maintaining the conditions. Support vector machine (SVM) is one such algorithm of ML used to train and classify the data. The present work uses the SVM for predicting the surface roughness in the end milling of the low-carbon steel. The experiments were performed at nine different combinations of process parameters. Moreover, to monitor the cutting process online, the current drawn is measured using a current sensor. In this regard, a correlation between the current drawn and variation in surface roughness is reported. The average value of the surface roughness was predicted using the SVM at each combination. The results show that the SVM estimates the surface roughness with an approximate error of 0.4 %-10%. On the other hand, the surface roughness variation does not fit well with the current signals due to the variation in tool wear.
52.	MAGIC-TBR: Multiview attention fusion for transformer-based bodily behavior recognition in group settings **S Madan, R Jain, G Sharma,** R Subramanian, **A Dhall** - MM '23: Proceedings of the 31st ACM International Conference on Multimedia, 2023 **Abstract:** Bodily behavioral language is an important social cue, and its automated analysis helps in enhancing the understanding of artificial intelligence systems. Furthermore, behavioral language cues are essential for active engagement in social agent-based user interactions. Despite the progress made in computer vision for tasks like head and body pose estimation, there is still a need to explore the detection of finer behaviors such as gesturing, grooming, or fumbling. This paper proposes a multiview attention fusion method named MAGIC-TBR that combines features extracted from videos and their corresponding Discrete Cosine Transform coefficients via a transformer-based approach. The experiments are conducted on the BBSI dataset and the results demonstrate the effectiveness of the proposed feature fusion with multiview attention. The code is available at: https://github.com/surbhimadan92/MAGIC-TBR.
53.	Mechanical behaviour of mild steel during multi-scan laser bending with forced cooling YP Sharma, **R Kant**, BS Sidhu, R Yadav - Optics & Laser Technology, 2023 **Abstract:** Laser bending is an innovative sheet metal forming technique. Researchers are focusing optimizing the process for enhancing bend angles and mechanical properties. To achieve this, a waiting period between laser scans is vital to re-establish the temperature gradient and improve bend angles. Forced cooling is a critical element in reducing this waiting time. This

	study investigates the influence of cooling environments (natural and forced cooling) during laser bending of mild steel sheets. It examines the impact of key parameters such as laser power, scan speed, and beam diameter under both cooling conditions. The results reveal that under forced cooling, specific combinations of process variables lead to exceptional outcomes. Notably, a bend angle of 8.81° is achieved with higher laser power (1000 W) and slower scan speed (1000 mm/min) in forced cooling condition. This study also analyzes temperature variations concerning laser power, scan speed, beam diameter, and the number of scans. Furthermore, under forced cooling conditions, an increase in ultimate tensile strength and micro-hardness is observed within the irradiated region. The highest micro-hardness value of 198.5 HV, was attained under forced cooling conditions at 1000 W of laser power and a scan speed of 1000 mm/min. This research underscores the potential of forced cooling mechanisms to significantly enhance laser bending outcomes, encompassing both bend angles and material properties.
54.	Metal- and additive-free TfOH catalyzed chemoselective O- and S-trifluoroethylation of oxindoles, isoindolines and thio-oxindoles **M Lamba, PR Singh, S Bhatt, A Goswami** - Green Chemistry, 2023 **Abstract:** Fluorine-containing moieties are of great interest in the development of new synthetic methods due to their considerable medicinal value. Thus, researchers have explored direct trifluoroethylation using CF_3CH_2-containing precursors; however, the high cost, prolonged synthesis time, toxic nature, and instability towards transition metal catalysis of these precursors pose challenges. As an alternative, conducting trifluoroethylation by *in situ* production of 2,2,2-trifluorodiazoethane (CF_3CHN_2) from $CF_3CH_2NH_2$·HCl in solution is a comparatively easy, safe, and greener approach. However, previous reports using 2,2,2-trifluorodiazoethane in solution also demonstrate the use of transition metal-catalyzed pathways under harsh reaction conditions and hazardous solvents. Herein, we have developed a triflic acid (a commercially available and cheap Brønsted acid) catalyzed protocol for *O*-trifluoroethylation of 3,3-disubstituted, monosubstituted, unsubstituted, and chalcone-based oxindoles and isoindolines, and *S*-trifluoroethylation of thio-oxindoles in the presence of *in situ* generated 2,2,2-trifluorodiazoethane in solution. This highly efficient metal- and additive-free strategy offers a mild and feasible approach to achieve chemoselective trifluoroethylation with good to excellent yields in a very short reaction time (10 minutes). This methodology has a broad substrate scope, making it a versatile approach that can be effectively employed for all types of cyclic amides. Additionally, the method is scalable for larger operations. The calculation of various green chemistry metrics, such as high atom economy (93%), high carbon efficiency (100%), high reaction mass efficiency (74%), and low E-factor(0.40 kg waste per kg product), confirms the eco-friendliness of this approach. The EcoScale evaluation showcases the simplicity, effectiveness, and eco-friendliness of this approach. 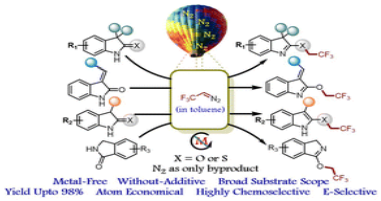
55.	Metal surface engineering for extreme sustenance of jumping droplet condensation M Donati, K Regulagadda, … **CS Sharma**… - Langmuir, 2023 **Abstract:** Water vapor condensation on metallic surfaces is critical to a broad range of applications, ranging from power generation to the chemical and pharmaceutical industries. Enhancing simultaneously the heat transfer efficiency, scalability, and durability of a condenser surface remains a persistent challenge. Coalescence-induced condensing droplet jumping is a capillarity-driven mechanism of self-ejection of microscopic condensate droplets from a surface.

	This mechanism is highly desired due to the fact that it continuously frees up the surface for new condensate to form directly on the surface, enhancing heat transfer without requiring the presence of the gravitational field. However, this condensate ejection mechanism typically requires the fabrication of surface nanotextures coated by an ultrathin (<10 nm) conformal hydrophobic coating (hydrophobic self-assembled monolayers such as silanes), which results in poor durability. Here, we present a scalable approach for the fabrication of a hierarchically structured superhydrophobic surface on aluminum substrates, which is able to withstand adverse conditions characterized by condensation of superheated steam shear flow at pressure and temperature up to ≈1.42 bar and ≈111 °C, respectively, and velocities in the range ≈3–9 m/s. The synergetic function of micro- and nanotextures, combined with a chemically grafted, robust ultrathin (≈4.0 nm) poly-1*H*,1*H*,2*H*,2*H*-perfluorodecyl acrylate (pPFDA) coating, which is 1 order of magnitude thinner than the current state of the art, allows the sustenance of long-term coalescence-induced condensate jumping drop condensation for at least 72 h. This yields unprecedented, up to an order of magnitude higher heat transfer coefficients compared to filmwise condensation under the same conditions and significantly outperforms the current state of the art in terms of both durability and performance establishing a new milestone. 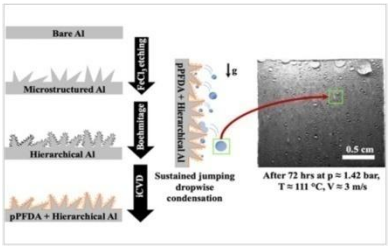
56.	Minimalism: a game changer for industries **Amritesh, A Kaur** - Sustainable Consumption Experience and Business Models in the Modern World: Book Chapter, 2024 **Abstract:** Minimalism has become a lifestyle choice for consumers from various cultural backgrounds who are deliberately rejecting the consumerist narratives that drive market-driven lifestyles. This chapter aims to provide a comprehensive review of growing trends in minimalism, emphasizing the defining traits of minimalists, the historical origins of minimalism, and the potential risks it poses to deindustrialization. A bibliographic review method is used to address the interconnected concepts within the specified objectives. The study illuminates the global shift in consumer behaviour by examining the increasing embrace of minimalism in different consumer sectors of the economy. The authors highlight the disruptive capacity of minimalism in various industries and recommend further research to plan a systematic degrowth of unsustainable products and match it with the emerging demand for a minimalism-driven lifestyle. In summary, this chapter emphasizes the potential connections among minimalism, health and wellbeing, and environmental sustainability.
57.	Modeling dropwise condensation on hydrophobic microgrooved surface **S Bahal, CS Sharma** - Langmuir, 2023 **Abstract:** Dropwise condensation heat transfer on water-repellent surfaces is inherently linked to the mode of droplet departure from the surface. When a microgrooved hydrophobic surface is exposed to condensation, multiple spontaneous droplet removal pathways for surface renewal are manifested. We present numerical modeling of dropwise condensation on a microgrooved hydrophobic surface. Our model is an extension of the well-established one-dimensional modeling approach involving estimation of overall condensation heat transfer through the integration of individual droplet contributions. The model presented here accounts for all the surface renewal mechanisms observed on the microgrooved hydrophobic surface: growth and coalescence of condensate droplets within the microgroove and on the ridges, imbibition of the

	microgrooves with condensate, bulge formation, spontaneous dewetting of the microgrooves, and shedding of large drops through gravity. The modeling results show that the microgrooves trigger condensate shedding from the surface much earlier compared to a planar hydrophobic surface. As a result, the microgrooved hydrophobic surface maintains a much lower area coverage and attains a significantly higher condensation heat flux compared to a planar surface. The model also enables isolation of the relative contributions of the four mechanisms, wherein it is observed that the spontaneous dewetting transition of microgrooves dominates the other mechanisms in terms of the overall surface renewal rate. This is in contrast to the planar hydrophobic surface where droplet shedding under gravity is the main surface renewal mechanism. Finally, we also evaluate the effect of microgroove geometry on the condensation heat transfer performance. The model predicts that hydrophobic microgrooves with depth of ~200 μm and narrow widths below ~100 μm can yield enhanced thermal performance. 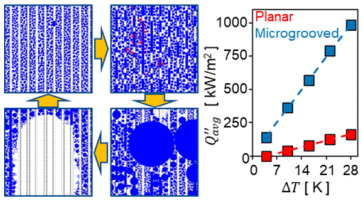
58.	Nonlinear load time-constant based filter inductance design for PV-driven grid-connected SAF/PFC in EV charging infrastructure **PM Reddy**…**KR Sekhar, BK Gupta** - 49th Annual Conference of the IEEE Industrial Electronics Society, 2023 **Abstract:** The objective of this work is to emphasize the impact of load time constant in designing the terminal inductance of a Photo-Voltaic (PV) driven grid-connected inverter. The inverter is intended for feeding non-linear load in Electric vehicle (EV) charging infrastructure. Unlike conventional Power Factor correction (PFC) or Shunt Active Filter(SAF), the inverter-based source delivers fundamental and harmonic current components per system requirements. Hence, it is essential to consider the equivalent system seen by the inverter-based source to accomplish its operational modes while acting as a source of fundamental power, SAF, or both. The mathematical formulation associated with the inductor design for both the conventional and proposed approaches is presented. Additionally, the necessity of auto controller gain adjustment to facilitate seamless power injection along with the nonlinear load harmonics at various loading conditions is demonstrated. The filter design methodology, along with the nonlinear load harmonic compensation mechanism, is evaluated through experimental results.
59.	Numerical investigation of transitional mixed convection for buoyancy-assisting and opposing flows in a vertical tube **S Gorai**, **D Samanta**, SK Das - International Heat Transfer Conference 17, 2023 **Abstract:** This numerical study investigates the heat transfer, pressure drop, and flow characteristics for buoyancy-assisting and opposing flow of water in the simultaneously hydrodynamically and thermally developing laminar-turbulent transitional regime of mixed convection in a vertical tube. Two-dimensional axisymmetric steady-state simulations were carried out for Reynolds number (*Re*) from 2000 to 5000, Grashof number (*Gr*) from 4×10^5 to 2.5×10^6, and Richardson number (*Ri*) 0.1 with a length-to-diameter (*L/D*) ratio of 150, subjected to constant heat flux boundary condition from the tube walls. Numerical simulations were performed using the pressure-velocity coupling scheme and second-order UPWIND scheme for momentum, energy, and other transport quantities. Two transition models have been compared, and the model with the better performance, known as the Transition Shear Stress Transport (SST), is used for the simulations. Results show that buoyancy plays a significant role in laminar-turbulent transition in assisting and opposing flows. The pressure drop and heat transfer increases with the increase in *Re* at fixed *Ri* in both the flows. In addition to it, at a given *Ri*, the pressure

	drop as well as heat transfer both are higher in opposing flow. The effect of heat flux on the entry length is also analyzed in buoyancy-assisting and opposing flow. It decreases in both the flows with the increase of heat flux. Furthermore, the start of transition depends on the heat flux supplied and it gets delayed with the increase of it.
60.	Numerical validation of fatigue properties and investigation of local deformation of heat-affected zones in P91 steel's weld joint R Dhiman , **SC Roy**, K Mariappan… - International Journal of Fatigue, 2023 **Abstract:** The low cycle fatigue (LCF) behavior of P91 steel weld joint (WJ), prepared by gas tungsten arc welding, has been investigated both experimentally and numerically. However, due to the smaller size and complex geometry of various zones of the WJ, the experimental investigation of the local fatigue behavior of different sub-regions of the heat-affected zones (HAZ) could not be made. Hence, the sub-regions of the WJ were reproduced at bulk scale by physical-thermal simulation (PTS) (i.e., heat treatment) to study the LCF behavior of the individual zones of P91 WJ. In the literature, the accuracy of such physical-thermally simulated bulk-scale specimens, which correspond to different sub-regions in the weld joint, is confirmed by comparing the microstructures and microhardness. In this article, a new method, based on the LCF experiment and finite element simulation, is proposed to validate the PTS method and the fatigue properties of the sub-regions of the weld joint. The simulation accurately predicted the failure location and also the most vulnerable sub-region within the WJ, as observed experimentally. Moreover, significant ratcheting and heterogeneous deformation were observed in the sub-regions of the WJ. 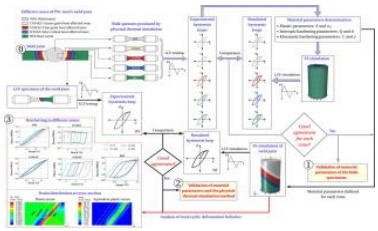
61.	Nutrient enrichment and phytoplankton toxicity influence a diversity of complex dynamics in a fear-induced plankton-fish model **A Mandal**…S Biswas - Journal of Theoretical Biology, 2023 **Abstract:** In this paper, we contemplate the dynamics of an aquatic system consisting of three interacting species, phytoplankton, zooplankton, and fish. We assume that the evading risk of fish predation induces fear in zooplankton species, which affects its growth dynamics radically. On the other hand, zooplankton develop an anti-predator defense by taking temporary refuge. Interestingly, the system potentially exhibits multi-stable configurations under identical ecological conditions by allowing different bifurcation scenarios, including multiple saddle–node and transcritical bifurcations with varying levels of nutrients, strength of phytoplankton toxicity, zooplankton refuge size and the cost of fear imposed by fish population. Further, by adding Gaussian white noise, we have extended the deterministic system to its stochastic version. We find that white noise appears to regulate the survival and extinction of model species. Comprehensive numerical simulations are consistent with mathematical results prognosticated by linear analysis. Overall, our study may provide a new insight into the mechanisms of emergence and mitigation of plankton blooms.
62.	Parallel active charge balance technique of li-ion batteries using combined phase shifted and boost DC-DC Converter **A Ahmad**, V Singh, **AV Ravi Teja, S Payami** - 49th Annual Conference of the IEEE Industrial Electronics Society, 2023 **Abstract:** Cell balancing in Li-ion batteries is a very crucial task considering the effective loss of

	unusable charge that remains in the cells when one or more cells of the pack loses charge. The main idea of the cell balancing is to achieve a state of charge among cells where minimum or no charge of the battery remains unused while discharging and none of the cells overcharge in a response to charge the weaker cell to the full capacity. Several active cell balancing methods are available that mainly focus on same limb or string cells balancing. In this article focus is made on charge transfer among parallel strings of the battery using combined Phase shifted and boost dc converters. The proposed cell balancing is very efficient in parallel charge balancing and can improve over all balancing efficiency of the BMS in achieving both same and parallel limb balancing. The proposed topology has been evaluated using MATLAB/Simulink with the help of inbuilt Li-ion NMC cell model (3.7V, 2.050Ah) and the results are presented.
63.	Parallel governing criteria for non-Newtonian droplet rebound suppression on superhydrophobic surfaces K Kamaluddin, GC Pal, P Dhar, **CS Sharma, S Samanta** - Colloids and Surfaces A: Physicochemical and Engineering Aspects, 2023 **Abstract:** Non-Newtonian droplets are known to suppress rebound on superhydrophobic (SH) surfaces. Our previous work (Dhar et al., Phys Rev Fluids, 2019, vol 4 [1]) showed that the polymer concentration and impact velocity must exceed a certain threshold to initiate the onset of rebound suppression. Analogous to drag reduction or elastic instabilities, we proposed that rebound suppression occurs only when the Weissenberg number exceeds 1 (Wi >1) at the onset of retraction. In this study, we explore four different types of SH surfaces to examine the universality of the previous observation (the importance of Wi >1 for rebound suppression). We observed that rebound suppression does not occur on all types of SH surfaces. The surfaces where rebound suppression was observed are categorized as '*Type-I*', while the remaining as '*Type-II*'. The non-uniformity in the rebound suppression phenomena is explained by the role of Cassie to Wenzel transformation (CWT) or impalement. We showed that for '*Type-I*' surfaces, when the ratio of dynamic pressure (P_D) to minimum capillary pressure (P_C) becomes $P_D/P_C > 1$, the rebound is suppressed. The '*Type-II*' surfaces have characteristic spacing in the order of nanometers, which is three orders of magnitude lower than the microtextured *'Type-I'* surface. Thereby, the capillary pressure is significantly higher for *'Type-II'*. The dynamic pressure could not surpass the capillary pressure for the impact velocities and polymer concentrations studied for the *'Type-II'* surface. As P_D/P_C remained < 1, for 'Type-II' surfaces, rebound suppression was not observed. It must be noted that for the same values of $P_D/P_C > 1$ values, water droplets didn't show rebound suppression on *'Type-I'* surfaces. The non-Newtonian droplets are known to slow down the retraction dynamics due to normal stress, extensional viscosity and higher adsorption at the substrate. We have demonstrated the role of extensional viscosity in this study, particularly how strain stiffening of radial filaments emanating from the droplet aids in dissipating energy, which further arrests drop rebound. Therefore, the existence of two parallel mechanisms: the role of fluid elasticity (manifested through $Wi > 1$), and $P_D/P_C > 1$, are necessary for the rebound suppression.
64.	Peak floor acceleration demands in torsionally irregular buildings **A Jain**, **M Surana** - Earthquake Engineering & Structural Dynamics, 2023 **Abstract:** Accurate estimation of the peak floor acceleration (PFA) plays a crucial role in ensuring the seismic safety of a building, its contents, and attachments. This study investigates amplification in PFA due to building torsion. Torsionally irregular reinforced-concrete moment-resisting frame buildings are analyzed under bidirectional earthquake excitations for five levels of ductility demands. A total of 5600 nonlinear dynamic analyses are conducted on the considered buildings while subjected to the far-field ground motions suite. It is shown that the existing code provisions significantly underpredict the PFA demands at the flexible edge of elastic and moderately inelastic torsionally irregular buildings. The torsional amplification factors

	for PFA demands depend on the building's torsional and strength characteristics. Further, these torsional amplification factors are correlated well with the building's elastic floor displacement-based torsional irregularity indices. Practice-oriented equations are proposed to predict the torsional amplification factors for PFA demands in torsionally irregular buildings. The proposed equations can be easily used after estimating the elastic floor displacement-based torsional irregularity indices using the modal superposition method. When applied with the latest ASCE 7 provisions, the proposed equations provide reasonably accurate estimates of the PFA demands in torsionally irregular buildings.
65.	Polymorphism-driven distinct nanomechanical, optical, photophysical, and conducting properties in a Benzothiophene-quinoline. KS Bejoymohandas, **A Redhu**…**RV Nair** … - Chemistry- A European Journal, 2023 **Abstract:** Polymorphic forms of organic conjugated small molecules, with their unique molecular shapes, packing arrangements, and interaction patterns, provide an excellent opportunity to uncover how their microstructures influence their observable properties. Ethyl-2-(1-benzothiophene-2-yl)quinoline-4-carboxylate (BZQ) exists as dimorphs with distinct crystal habits - blocks (BZB) and needles (BZN). The crystal forms differ in their molecular arrangements - BZB has a slip-stacked column-like structure in contrast to a zig-zag crystal packing with limited π-overlap in BZN. The BZB crystals characterized by extended π-stacking along [100] demonstrated semiconductor behavior, whereas the BZN, with its zig-zag crystal packing and limited stacking characteristics, was reckoned as an insulator. Monotropically related crystal forms also differ in their nanomechanical properties, with BZB crystals being considerably softer than BZN crystals. This discrepancy in mechanical behavior can be attributed to the distinct molecular arrangements adopted by each crystal form, resulting in unique mechanisms to relieve the strain generated during nanoindentation experiments. Waveguiding experiments on the acicular crystals of BZN revealed the passive waveguiding properties. Excitation of these crystals using a 532 nm laser confirmed the propagation of elastically scattered photons (green) and the subsequent generation of inelastically scattered (orange) photons by the crystals. Further, the dimorphs display dissimilar photoluminescence properties; they are both blue-emissive, but BZN displays twice the quantum yield of BZB. The study underscores the integral role of polymorphism in modulating the mechanical, photophysical, and conducting properties of functional molecular materials. Importantly, our findings reveal the existence of light-emitting crystal polymorphs with varying electric conductivity, a relatively scarce phenomenon in the literature.
66.	Quantification of pore accessibility in mesoporous supercapacitor electrode using cyclic voltammetry K Chatterjee, **PK Agnihotri**, S Basu… - IEEE Transactions on Instrumentation and Measurement , 2023 **Abstract:** Electrochemical double-layer capacitors (EDLCs) are energy storage devices that provide power densities higher than conventional batteries. Porosity and mass loading of the electrodes in an EDLC play crucial roles in determining its performance. The effective area accessible to the electrolyte may be orders of magnitude larger than the geometric area of the capacitor, largely due to the porous nature of the electrode. However, while the need to increase the effective area is well understood, measuring it is difficult. In this work, the voltage dependence of the double layer is proposed as a measure of the accessibility of the pore structure, and hence the effective area. Further more, a novel methodology is proposed to isolate the capacitance of the double layer from the total capacitance obtained, using cyclic voltammetry (CV) measurements. This requires correction of the CV curve for Faradaic currents to avoid overestimation of the double-layer capacitance. The results also indicate that a targeted combination of power and energy densities can be achieved by carefully adjusting the mass loading.

67.	Rapid removal of methylene blue and tetracycline by rough particles decorated with Pt nanoparticles **F Khan, C Shekhar, T Mondal, M Sabapathy** - Journal of Nanoparticle Research, 2023 **Abstract:** The increasing groundwater pollution resulting from industrial dyes and pharmaceutical products, which come from various sources, requires urgent attention to implement effective remediation measures. We demonstrate that the rough particles studded with platinum (Pt) nanoparticles can be fabricated at room temperature straightforwardly and in a single step. These rough particles displayed a good catalytic power (100% removal efficiency) against a model industrial dye (methylene blue) and pharmaceutical residue (tetracycline) within a reasonable time scale. Characterization techniques such as X-ray diffraction (XRD), atomic force microscopy (AFM), and field emission scanning electron microscopy (FESEM) confirmed the uniform deposition of Pt nanoparticles on the surface of polystyrene particles, forming dense islands and the roughened surface. Further, we investigated the influence of particle size, concentration, and contact patterns on the performance of rough catalytic particles. The semi-batch conditions favoured the complete decomposition of tetracycline within 40 min, but the batch-wise operation offered a good contacting pattern for methylene blue, yielding a maximal output within 10 min. The kinetics of the heterogeneous catalytic process modelled by Langmuir-Hinshelwood kinetics (r = k KC/1 + KC) predicts that the given methylene blue decomposition reaction induced by the rough particles follows the pseudo-first-order kinetics. The rate constants for the reaction catalyzed by 0.6 and 1.0 m-sized rough particles are 0.048 and 0.032 min−1, respectively. Furthermore, we established the proof-of-concept using magnetically responsive nanoparticles for real-time applications, including decontamination and recovery of catalyst particles via an externally applied magnetic field in one cycle. Our proposed method helps achieve a near-100% degrading efficiency within 10 to 40 min at minimal catalytic particle concentration, i.e., 200 ppm. Since we can turn the rough particles into super-paramagnetic, we can recover and reuse them for several wastewater treatment cycles without incurring running costs.
68.	Real-time serviceable path planning using uavs for waterborne vehicle navigation during floods **A Garg, SS Jha** - Proceedings of the 2023 6th International Conference on Advances in Robotics, 2023 **Abstract:** Autonomous navigation and formation control of multi-UAV systems pose a significant challenge for the robotic systems that operate in partially observable, dynamic and continuous environments. This paper addresses the problem of multi-UAV cooperative sensing and coverage of a flood-struck region to identify serviceable paths to critical locations for waterborne vehicles (WBV) in real time. A serviceable path is defined as a location that is obstacle free and has adequate water level for possible movement of WBVs. We develop a deep reinforcement learning model to learn a cooperative multi-UAV policy for real-time coverage of a flooded region. The coverage information gathered by the UAVs captures the presence of obstacles present in the path connecting the start and target/critical locations given by the shortest Manhattan distance. This coverage information is utilized by the path planning algorithm, i.e., MEA*, to minimize the number of expansion nodes and identify a serviceable path quickly. To conserve energy, UAVs initially follow a guided path to explore the optimal route. If obstacles are encountered, the UAVs search nearby areas for an alternate path to reach the critical location(s). The proposed approach, MEA* MADDPG, is compared with other prevalent techniques from the literature over real-world inspired simulated flood environments. The results highlight the significance of the proposed model as it outperforms other techniques when compared over various performance metrics.
69.	Robotic path planning for direct slicing method to minimize support structure in fused filament fabrication process **S Sharma, E Singla, R Kant** - Proceedings of the 2023 6th International Conference on

	Advances in Robotics, 2023 **Abstract:** This paper presents a path planning strategy for 3D printing using the Robot-assisted Fused Filament Fabrication (FFF) process. The strategy enables non-planar and non-uniform material deposition on both planar and non-planar surfaces, in contrast to traditional methods which deposit layers horizontally on a flat surface using a.stl file. The proposed strategy involves outer-layer and inner-layer path planning, resulting in a reduction in support structure requirements in the FFF process. Additionally, the use of direct slicing instead of slicing a.stl file leads to a more accurate final object. This approach demonstrates a novel method for 3D printing and path planning. In order to achieve the desired properties of an object, one can explore the realm of possibilities by skillfully manipulating printing parameters.
70.	Robotic tool-path generation for complex and overhang-angled parts through offline programming **S Rathor, S Kumar, E Singla, R Kant, CK Nirala** - AIR '23: Proceedings of the 2023 6th International Conference on Advances in Robotics, 2023 **Abstract:** This study presents the applicability of the offline programming a professional robotic arm to generate the nozzle path for complex and small overhang angled (OA) geometry parts. The software environment considers the wire-feed robotic laser additive manufacturing (WRLAM) experimental setup to introduce offline programming for complex shapes parts and parts with smaller overhang angles. The experimental setup consists of a KUKA KR6, 6-DOF robotic manipulator with a laser head attached to the end-effector of robotic arm. This setup has a customized wire feeder to incorporate wires with different sizes. The wire is fed to the nozzle of the laser head using a hose pipe for laser-wire interaction. This study includes the simulation of the robot travel path using path command and python script approach to generate program files for the process. The proposed approach will help to study the better performance of AM and welding processes in a lab environment and overcome challenges while performing experiments.
71.	Selection and thermophysical assessment of phase change materials (PCMs) for space cooling applications in buildings **PJ Abass, S Muthulingam** - Numerical Heat Transfer, Part A: Applications, 2023 **Abstract:** Phase change materials are gaining more attention in building comfort applications because of their latent heat thermal energy storage (TES) capacity. Identifying the best PCM candidate is a pivotal factor that significantly impacts the thermal performance of a building. This study delves into assessing prospective PCM candidates for potential utilization in cooling systems within buildings in hot subtropical climates. Extending the application of multicriteria decision-making (MCDM) methodologies, this research scrutinizes various commercial PCMs by conducting an exhaustive analysis of pertinent literature in the context of this specific application objective. Thermophysical properties are integrated into the MCDM framework to identify the most fitting candidates with optimal properties and attributes. The properties and attributes of PCMs are subjected to scoring and weighting through the AHP based on their significance in the given application context. TOPSIS and VIKOR techniques select the suitable PCM from the identified PCMs. The results showed that latent heat receives the highest weightage, amounting to 50.2%, due to its paramount importance. Furthermore, OM37 emerged as a promising choice for building space cooling, considering the prescreened temperature range of 30 °C–40 °C and for the specific location under consideration. Following PCM selection, thorough characterization was performed to evaluate the suitability of the chosen PCM for integration within building envelopes. The thermal conductivity of OM37 was determined to be 0.20 W/mK, while the morphology by a Field Emission Scanning Electron Microscope (Fe-SEM) intricate porous structure. Furthermore, a differential scanning calorimeter (DSC) suggests melting and solidification temperatures of 40 °C and 34 °C with a total enthalpy of 197.04 j/g, and a

	Thermogravimetry Differential Thermal Analysis (TG/DTA) showed a substantial weight loss of approximately 98.9% at around 247.3 °C. The presented experimental test results agree with the literature data and other researchers' results.
72.	Selective harmonic elimination PWM technique based on higher order sliding modes: generalized formulation **P Kalkal, AV Ravi Teja** - IEEE Journal of Emerging and Selected Topics in Power Electronics, 2023 **Abstract:** This paper pioneers a novel selective harmonic elimination (SHE) technique employing second-order sliding mode control. Unlike conventional methods, the proposed method leverages second-order sliding mode control to tackle the nonlinear equations of SHE, yielding smooth switching angles devoid of chattering. Theoretical analysis, including detailed derivations of controller parameters ensuring convergence, is presented. The algorithm has minimal computational burden, making it both simple to implement and robust in achieving convergence for any given modulation index. Simulation results, conducted in MATLAB/Simulink, and corresponding hardware outcomes from an FPGA-based experimental prototype in the laboratory validate the efficacy of the proposed algorithm. The proposed algorithm achieves the computation of switching angles in under 1.5 μs for a configuration involving five switchings per quarter.
73.	Selective hydrogenation of cinnamaldehyde, furanic, and aromatic aldehydes over a Z-scheme heterojunction photocatalyst constituted of Pd NPs Supported on g-C_3N_4/ZnO Nanocomposite **R Ghalta, A Chauhan**, **R Srivastava** - ACS Applied Nano Materials, 2023 **Abstract:** In this study, a Z-scheme heterojunction photocatalyst is fabricated by systematically manipulating and integrating g-C3N4 and ZnO. The Z-scheme g-C3N4(x)/ZnO(y) exhibits enhanced charge separation and migration, confirmed through photoluminescence (PL), time-correlated single-photon counting spectroscopy, and electrochemical impedance spectroscopy. Pd NPs, with an elevated work function and low Fermi energy level, are decorated onto the heterojunction, further amplifying charge separation, as revealed by ultraviolet photoelectron spectroscopy. The resulting Pd-decorated photocatalysts (Z%Pd@g-C3N4(x)/ZnO(y)) are evaluated for the selective reduction of α–β unsaturated compound, cinnamaldehyde. The catalysts with lower Pd NPs (0.5 or 1%) afford ∼100% yield for hydrocinnamaldehyde, while higher Pd NPs (3%Pd@g-C3N4(0.73)/ZnO(0.27)) afford ∼100% yield for hydrocinnamyl alcohol. Biomass-derived furanic aldehydes afforded ring-reduced and side-chain-reduced products under different Pd loading, whereas no ring-reduced products were obtained for the aromatic aldehydes. Interface interactions impact charge migration, leading to longer lifetimes for photogenerated charge pairs and improved separation of electrons and holes in photocatalytic processes. Characterizations and control experiments provide valuable insights into the structure–activity relationship, ultimately contributing to formulating a plausible reaction mechanism for photocatalytic reduction. 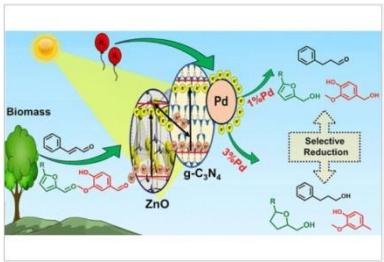
74.	Synchronization of three-phase grid-connected inverter using second-order sliding mode controller **T Bharti, AV Ravi Teja, J. Kalaiselvi** - 49th Annual Conference of the IEEE Industrial

	Electronics Society, 2023 **Abstract:** This article presents Second-Order Sliding Mode Control (SOSMC) to synchronize the three-phase grid-tied inverter and discuss the existing problem in the synchronization process through conventional PLL schemes and so to eliminate the problems related to the PLL the proposed PLL-less strategy employ the Second-Order Sliding Mode Controller, the suggested controller is implemented in stationary reference frame (alpha-beta reference frame) to eliminate the need for PLL and since Park's transformation is also not required the computational burden is also reduced in this approach, further the proposed model is compared with the existing PLL-less strategy and the results shows the effectiveness of the proposed method in reducing the power ripples and keeping the system stable even in unbalanced conditions.
75.	Tailoring cellulose paper via electroless CuSnB deposition for selective electrochemical detection of dopamine **A Kafle, D Gupta, D Mehta, TC Nagaiah** - ChemComm, 2023 **Abstract:** A novel, biodegradable substrate based, and cost-effective flexible electrochemical sensor was developed for the highly selective and sensitive detection of one of the major neurotransmitters, dopamine, which can be utilised as a disposable electrode for point-of-care diagnostic applications. The active material CuSnB decorated over cellulose paper exhibits good sensitivities of 3.92 μA μM−1 cm−2 with a limit of detection of 0.5 nM. Moreover, the flexible sensor demonstrated superior selectivity towards co-existing metabolites such as ascorbic acid, glucose, and uric acid, in addition to stability at various mechanical deformations.
76.	The role of osteogenic effect and vascular function in bone health in hypertensive rats: a study of anti-hypertensive and hemorheologic drugs S Pal…**S Kumar, N Kumar**… - Calcified Tissue International and Musculoskeletal Research, 2023 **Abstract:** Vascular dysfunction contributes to the development of osteopenia in hypertensive patients, as decreased blood supply to bones results in tissue damage and dysfunction. The effect of anti-hypertensive medicines on bone mass in hypertensive individuals is inconclusive because of the varied mechanism of their action, and suggests that reducing blood pressure (BP) alone is insufficient to enhance bone mass in hypertension. Pentoxifylline (PTX), a hemorheological drug, improves blood flow by reducing blood viscosity and angiogenesis, also has an osteogenic effect. We hypothesized that improving vascular function is critical to increasing bone mass in hypertension. To test this, we screened various anti-hypertensive drugs for their in vitro osteogenic effect, from which timolol and hydralazine were selected. In adult female spontaneously hypertensive rats (SHRs), timolol and hydralazine did not improve vascular function and bone mass, but PTX improved both. In female SHR animals, PTX restored bone mass, strength and mineralization, up to the level of normotensive control rats. In addition, we observed lower blood vasculature in the femur of adult SHR animals, and PTX restored them. PTX also restored the bone vascular and angiogenesis parameters that had been impaired in OVX SHR compared to sham SHR. This study demonstrates the importance of vascular function in addition to increased bone mass for improving bone health as achieved by PTX without affecting BP, and suggests a promising treatment option for osteoporosis in hypertensive patients, particularly at-risk postmenopausal women.
77.	Thermal monitoring and deep learning approach for early warning prediction of rock burst in underground structures **M Jaiswal, R Sebastian**, R Mulaveesala - Journal of Physics D: Applied Physics, 2023 **Abstract:** The occurrence of rockburst has the potential to result in significant economic and human losses in underground mining and excavation operations. The accuracy of traditional

	methods for early prediction is considerably affected by factors such as site conditions, noise levels, accessibility, and other variables. This study proposes a methodology for identifying the most defected region in a hard rock sample by integrating motion thermogram data obtained from the laboratory monitoring of rock burst phenomena with a cutting-edge deep neural network approach based on a regional convolutional network (i.e. Mask RCNN). The efficacy of the suggested approach was evaluated by determining the F1 score and average precision matrices based on a specific intersection over union value. The findings demonstrate that the proposed approach possesses satisfactory precision with respect to detection, localization, and segmentation, thereby establishing its potential utility as an autonomous predictor of rock bursts.
78.	Thermodynamic analysis of a hybrid novel solar powered humidification-dehumidification coupled with direct contact membrane distillation system KS Chauhan, R Beniwal, **H Tyagi** - Energy Conversion and Management, 2023 **Abstract:** Water scarcity is a well-known global issue, and obtaining potable water in many regions is challenging. Some technologies exist but require high-grade energy for freshwater production, which is not universally accessible. This work emphasizes desalinating saline water using low-grade energy, such as solar energy. The study introduced a novel design of hybrid solar-powered humidification-dehumidification coupled with direct contact membrane distillation (HDH-DCMD), including modeling heat transfer, mass transfer, and fluid flow. The obtained results are further validated against previously published findings. Additionally, a thermodynamic analysis of the hybrid system was conducted to examine the effects of several parameters, including variation in membrane area, top brine temperature (TBT), feed temperature, mass flow rate ratio (MR), and dimensions of the membrane module. The objective was to assess the influence of these factors on the overall distillate production, gain output ratio (GOR), and recovery ratio (RR). The hybrid system offers a significantly improved solution, yielding nearly double the distillate production and GOR compared to standalone HDH and DCMD systems. The performance of HDH and DCMD is interconnected, meaning that if one outperforms the other, the overall output remains constant. The overall distillate production remains unaffected by MR, while GOR is influenced by it, resulting in varying optimal points depending on the specific operating parameters. It has been observed that increasing the TBT results in an increase in distillate production, RR, and GOR. However, when the feed temperature increases, the distillate production and RR remain almost constant while the GOR continues to increase. 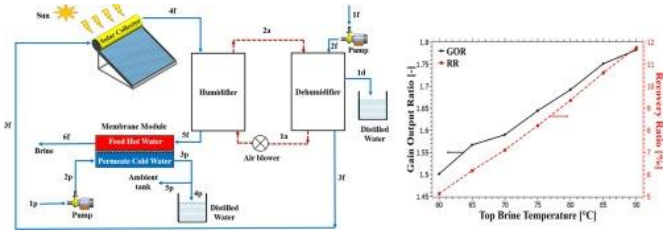
79.	Transient analysis and detection of terminal short circuit of medium frequency transformer in dual active bridge converter TJ Nistane, **K Jayaraman, S Payami** - 49th Annual Conference of the IEEE Industrial Electronics Society, 2023 **Abstract:** The dual active bridge (DAB) converter is a prominent topology in DC-DC power conversion. The SC fault across the transformer terminal of DAB converter may result in catastrophic failures. However, the existing literature lacks the details on analysis regarding transient performance of DAB with terminal short circuit (SC) faults. Thus, it is imperative to study the transient over current evaluation during terminal SC fault in transformer of DAB converter. In regard to the above concern, this paper gives the theoretical and experimental study of terminal faults in transformer. The detailed simulation study is carried out using

	MATLAB/Simscape and experimental results are shown using designed DAB prototype of 1 kW. Based on the analysis, a simple detection technique is proposed for terminal SC faults. This technique use the voltage across redundant winding coupled with the main winding of standalone leakage inductor and thereby reduce extra sensor cost for detection.
80.	Understand and quantify the consumers' cognitive behavior for the appropriateness features of product aesthetics through the eye-tracking technique **J Singh, P Sarkar** - International Journal on Interactive Design and Manufacturing (IJIDeM), 2023 **Abstract:** Product design goes beyond mere enclosure; it communicates a product's functionality and utilitarian features. A product's appeal, appropriateness, and beauty act as pivotal links between consumers and their choices. This study delves into the quantification of the appropriateness feature in product aesthetics and its profound influence on human visual and cognitive processes. Examining a diverse array of beverage bottle silhouettes, our two-phase study, involving six experts and over 300 participants, brings forth compelling revelations. In phase I, the Frequency Match Ratio (FMR) analysis underscores consumers' adept understanding of function perception during the visual matching of specific silhouettes. Notable examples include the remarkable match ratios achieved for alcohol bottle silhouette P2 (94.71%) and carbonated drink bottle silhouette P5 (85.88%). Furthermore, phase-II, the eye-tracking results revealed several significant findings. Gender-related differences in pupil diameter were noted, with males showing distinct variations, potentially influenced by the robust shapes of alcohol bottles, and females displaying fluctuations, suggesting familiarity with certain bottle designs, particularly under more complex tasks. The fixation count, a metric of cognitive processing, identified areas of pronounced interest influenced by shape, curvature, and texture, with female participants exhibiting distinct fixation patterns emphasizing the role of shape and curvature in evoking emotional responses. Total Fixation Duration, a measure of visual attention, indicated that participants allocated substantial time to examining angular and deeply curved shapes, particularly focusing on elements like bottle necks, slant heights, and angular regions. The study's findings provide designers with insights into consumer preferences for perception of function (appropriateness) feature of product aesthetics, enabling the creation of products that align with both form and function. This approach can empower companies to enhance product aesthetics and gain a competitive advantage.
81.	Unveiling the catalytic potential of two-dimensional boron nitride in lithium–sulfur batteries N Khossossi, D Singh…**R Ahuja** - Chemical Engineering Journal, 2023 **Abstract:** Lithium–sulfur (Li–S) batteries, renowned for their potential high energy density, have attracted attention due to their use of earth-abundant elements. However, a significant challenge lies in developing suitable materials for both lithium-based anodes, which are less prone to lithium dendrite formation, and sulfur-based cathodes. This obstacle has hindered their widespread commercial viability. In this study, we present a novel sulfur host material in the form of a two-dimensional semiconductor boron nitride framework, specifically the 2D orthorhombic diboron dinitride (o-$B2N_2$). The inherent conductivity of o-$B2N_2$ mitigates the insulating nature often observed in sulfur-based electrodes. Notably, the o-$B2N_2$ surface demonstrates a high binding affinity for long-chain Li-polysulfides, leading to a significant reduction in their dissolution into the DME/DOL electrolytes. Furthermore, the preferential deposition of Li2S on the o-$B2N_2$ surface expedites the kinetics of the lithium polysulfide redox reactions. Additionally, our investigations have revealed a catalytic mechanism on the o-$B2N_2$ surface, significantly reducing the free energy barriers for various sulfur reduction reactions. Consequently, the integration of o-$B2N_2$ as a host cathode material for Li–S batteries holds great promise in suppressing the shuttle effect of lithium polysulfides and

	ultimately enhancing the overall battery performance. This represents a practical advancement for the application of Li–S batteries.
82.	Viscous fingering instabilities in spontaneously formed blisters of MoS2 multilayers **M Pandey, R Ahuja, R Kumar** - Nanoscale Advances, 2023 **Abstract:** The viscous fingering in the Hele-Shaw cell can be suppressed by replacing the upper-bounding rigid plate with an elastic membrane. Recently, graphene multilayers while polymer-curing-induced blistering showed the dynamical evolution of viscous fingering patterns on a viscoelastic substrate due to their thickness-dependent elasticity. Under certain conditions, the elastic solid-based instability couples with the viscoelastic substrate-based instability. The mechanisms underlying such a coupling in the blisters of 2D materials and the dynamical evolution of the viscous fingering patterns underneath the blisters are yet to be addressed. Herein, we investigate the viscous fingering instabilities in spontaneously formed blisters of MoS2 multilayers, and provide thorough analytical and experimental insights for the elucidation of the dynamical evolution of the viscous fingering patterns and the coupled instabilities in the blisters. We also estimate the interfacial adhesion energy of the MoS2 flakes over a (poly)vinyl alcohol (PVA) substrate and the confinement pressure inside the MoS2 blisters using a conventional blister-test model. It is observed that the presence of instability gives rise to anomalies in the modeling of the blister test. The adhesion mechanical insights would be beneficial for fundamental research as well as practical applications of 2D material blisters in flexible optoelectronics. 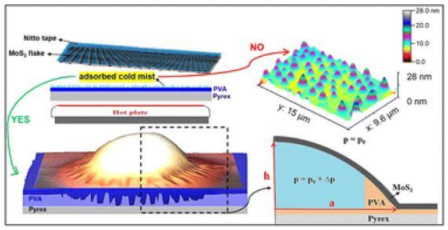
83.	Visible-light responsive azobenzene and cholesterol based liquid crystals as efficient solid-state solar–thermal fuels **AK KM, S Sony,** S Dhingra, **M Gupta** - ACS Materials Letters, 2023 **Abstract:** Solar–thermal fuels (STFs) based on photoresponsive molecules, which can harvest and store solar energy by the configurational change of molecules and can release it in the form of heat on demand, have been investigated recently. So far, azobenzene has been the most widely studied molecule for these applications. However, until now, only solid and liquid derivatives of azobenzene have been explored which suffer from several limitations. Here, we are reporting for the first time visible-light responsive STFs based on liquid crystals (LCs). We have prepared a series of compounds based on azobenzene and cholesterol with varying spacer and *ortho*-substitution on azobenzene. All of these derivatives exhibit enantiotropic chiral nematic (N*) mesophases. Moreover, they showed excellent photostability, photocyclability, and long half-life times of *cis*-states. We have further evaluated the thin films of these compounds for charging, i.e., *trans* to *cis* conversion under solar irradiation using various bandpass filters, and also studied the kinetics of the conversion. These compounds exhibited a maximum charging of up to 70% for the derivative with *ortho*-fluoro azobenzene. The charged thin films were further evaluated for their heat release properties by infrared (IR) thermal imaging. The maximum heat release observed was around 5.4 °C from the surrounding temperature which was significantly higher as compared to similarly substituted azobenzene-based derivative without a LC phase.

	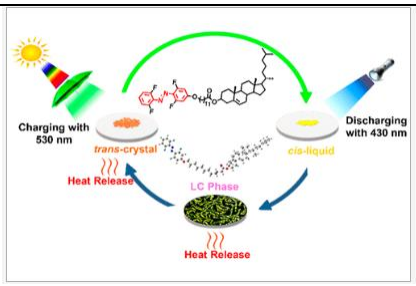
84.	Zirconium decorated 2D holey graphyne for high capacity hydrogen storage: Insights from first principles simulations **P Beniwal**, B Chakraborty, **TJD Kumar** - International Journal of Hydrogen Energy, 2023 **Abstract:** The hydrogen storage potential of a 2D analogue of graphyne, holey graphyne (HGY) monolayer decorated with the zirconium adatom is explored by the first-principles study. The Zr adatom exhibits a strong binding affinity on the HGY monolayer with −4.44 eV binding energy through an electronic charge transfer mechanism. Consequently, a localized spatial electrostatic field emerges around the Zr adatom and tends to result in the H molecules being adsorbed via the Kubas interaction. This interaction is due to back-and-forth charge transfer between the H-1s orbital and the Zr-4d orbital, resulting in a net charge gain by the H-1s orbital and leading to Hsingle bondH bond elongation. Furthermore, the high energy barrier for Zr diffusion over the HGY monolayer effectively averts the metal clustering concern. The thermal response of Zr-decorated HGY near room temperature and at elevated temperatures is examined via ab-initio molecular dynamics simulations. Each Zr adatom has the capacity to accommodate five hydrogen molecules, exhibiting adsorption energies spanning from −0.24 to −0.45 eV, leading to a notably high hydrogen weight percentage of 7.5, above the DOE's criterion of 5.5 wt%. This study validates the effectiveness of utilizing thermodynamically and energetically stable Zr-decorated HGY as an outstanding medium for hydrogen storage. 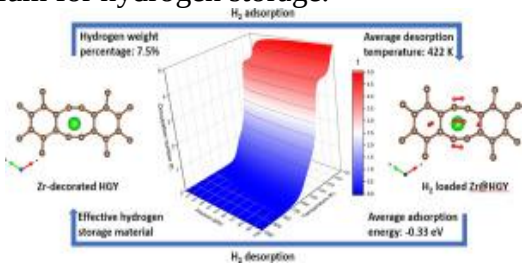

Disclaimer: This publication digest may not contain all the papers published. Library has compiled the publication data as per the alerts received from Scopus and Google Scholar for the affiliation "Indian Institute of Technology Ropar" for the month of December, 2023. The author(s) are requested to share their missing paper(s) details if any, for the inclusion in the next publication digest.